Frode Manstad-Hulaas

Navigation Technology in Endovascular Aortic Repair

Thesis for the degree of Philosophiae Doctor

Trondheim, March 2013

Norwegian University of Science and Technology
Faculty of Medicine
Department of Circulation and Medical Imaging

NTNU – Trondheim
Norwegian University of
Science and Technology

NTNU
Norwegian University of Science and Technology

Thesis for the degree of Philosophiae Doctor

Faculty of Medicine
Department of Circulation and Medical Imaging

SBN 978-82-471-4221-9 (printed ver.)
ISBN 978-82-471-4222-6 (electronic ver.)
ISSN 1503-8181

Doctoral theses at NTNU, 2013:62

Printed by NTNU-trykk

3D-bilder og navigasjon i endovaskulær aortabehandling

En rekke sykdommer kan ramme hovedpulsåren (aorta) og flere av disse kan behandles med endovaskulær (dvs. minimal invasiv) teknikk. Når hovedpulsåren skal repareres benyttes normalt røntgenstråler for å se hvor forskjellige instrumenter, som kateter (plastslanger), metalledninger, ballonger etc, befinner seg. Det kan også sprøytes kontrastvæske i aorta slik at denne fremstilles bedre på røntgenbildene. Bruk av kontrastvæske kan påføre enkelte pasienter nyresvikt. Mye røntegenstråler kan være helseskadelig og i tillegg er røntgenbildene bare 2-dimensjonale, dvs at man får ingen dybde i bildet. For å redusere bruken av røntgenstråler og kontrastvæske, samt å gi legene mulighet for en bedre romlig forståelse av kartreets anatomi under inngrepet, har vi undersøkt nytten av 3-dimensjonal visualisering og navigasjon. Dette har vært og er et samarbeid mellom Norges Teknisk-Naturvitenskapelige Universitet (NTNU) Inst. For Sirkulasjon og Bildediagnostikk, SINTEF Avd. For Medisinsk Teknologi og St Olavs Hospital ved Fremtidens Operasjonsrom. Et navigasjonssystem for blodårene har likhetstrekk med GPS-systemet som brukes i biler. Navigasjonssystemet kan angi posisjonen til forskjellige instrumenter i et 3-dimensjonalt bilde av blodåresystemet uten at røntgenstråler og kontrastvæske må benyttes. I fremtiden kan kanskje minimal invasiv behandling av hovedpulsåren utføres på en tryggere og mer presis måte ved hjelp av et navigasjonssystem.

Formålet med dette doktorgradsarbeidet var å undersøke om et navigasjonssystem med 3-dimensjonale bilder av blodåresystemet kan brukes i veiledning av

endovaskulær behandling av aorta og hvor nøyaktig et slikt navigasjonssystem er. Dette er undersøkt gjennom 4 delstudier.

Først ble det gjennom et modellforsøk vist at navigasjonssystemet kan benyttes for å sette inn en kunstig blodåre i hovedpulsåren. Ved hjelp av spesielt utviklet programvare kan røntgenbilder (CT-røntgen) av pasienten som er tatt før operasjonen benyttes som veikart (3-dimensjonalt bilde) for navigasjonssystemet. I både modell- og dyreforsøk ble det vist at posisjonen til instrumenter kan angis med stor grad av nøyaktighet ved hjelp av navigasjonssystemet. Til sist ble det i en pasientstudie vist at navigasjonssystemet også kan benyttes under innsetting av en kunstig blodåre i aorta.

Gjennom denne avhandlingen er det redegjort for at et navigasjonssystem som viser posisjonen til instrumenter i et 3-dimensjonalt bilde kan være et nyttig hjelpemiddel under minimal invasiv behandling av sykdommer i hovedpulsåren. Navigasjonssystemet har god nøyaktighet og er lett å bruke.

To my wife and sons

TABLE OF CONTENTS

1 ACKNOWLEDGEMENT

This work was carried out from 2005 to 2010 in the Operating Room of the Future, St Olavs Hospital, and the Department for Circulation and Medical Imaging, Faculty of Medicine, Norwegian University of Science and Technology (NTNU), in collaboration with SINTEF Department of Medical Technology and the National Centre of Competence in Ultrasound and Image Guided Therapy.

Primarily I wish to thank my supervisors: Petter Aadahl, Toril A Nagelhus Hernes and Torbjørn Dahl. You see problems from various angles and devise new approaches to solve them, and you provide insightful advice and suggestions. You have always been supportive, given structured feedback and pushed me forward.

I especially want to thank Geir Arne Tangen for our close, practical and productive collaboration

Furthermore, I wish to express my gratitude to:

- Stefanie Demirci
- Marcus Pfister
- Stian Lydersen
- Lucian Gheorghe Gruionu
- Hans Olav Myhre
- Asbjørn Ødegård
- Jenny Kristine Aasland
- Anne Karin Sjaastad
- Magnus Strømmen

- Andreas Seim
- Anne Karin Wik
- Ann Mari Kasseth
- Oddveig Lyng
- Kirsten Rønning

The study received funding from the Research Council of Norway through the FIFOS Program Project 152831/530, the FRIMED Program Project 196726/V50, the National Center of Competence for 3D Ultrasound in Surgery, SINTEF Dept. Medical Technology, the Norwegian University of Science and Technology and St Olavs Hospital.

2 SUMMARY

A number of diseases can affect the aorta, and endovascular (minimally invasive) techniques can be used to treat many of these conditions. During endovascular aortic repair, different instruments, such as catheters (plastic tubes), metal wires and balloons are visualized by X-rays. Intermittent aortic injections of contrast medium improve the depiction of the aorta; however, contrast medium may damage kidney function in some patients, radiation can be harmful and X-ray images are 2-dimensional, i.e., the impression of depth is missing. To reduce the use of X-rays and contrast medium, as well as to provide physicians with a better spatial understanding of a patient's vascular anatomy, one can use a navigation system with 3-dimensional images. The use of 3-dimensional visualization and navigation during the endovascular repair of aortic diseases is a subject of research at the Norwegian University of Science and Technology (NTNU), SINTEF Dept. of Medical Technology and St. Olav's Hospital. A navigation system for blood vessels has similarities to the GPS systems used in cars. Such a navigation system can provide the position of different instruments in a 3-dimensional image of a patient's vascular system without using X-rays and contrast medium. The use of a navigation system may improve precision and simplify future minimally invasive treatment of the aorta.

The purpose of this thesis was to investigate the applicability of a navigation system with 3-dimensional images of the vascular system for guidance in endovascular aortic treatment, and to assess the reliability of such a navigation system. The assessment was conducted in four sub-studies.

First, we used the navigation system to insert an endoprosthesis (artificial blood vessel) into a model of the abdominal aorta. With specially developed software, the navigation system can use 3-dimensional images (CT scans) of the patient acquired before the procedure as a roadmap. In phantom and animal experiments, the navigation system specified the position of instruments with a high degree of accuracy. Finally, we used the navigation system during the insertion of aortic endoprostheses in patients.

In this thesis, we demonstrate that a navigation system that enables visualization of instruments in a 3-dimensional image can be a useful tool during minimally invasive treatment of the aorta. The navigation system is accurate and easy to use.

3 LIST OF ORIGINAL PAPERS

1. **Manstad-Hulaas F**, Ommedal S, Tangen GA, Aadahl P, Hernes TN. Sidebranched AAA stent graft insertion using navigation technology – a phantom study. Eur Surg Res. 2007;39(6):364-71.
2. **Manstad-Hulaas F**, Tangen GA, Demirci S, Pfister M, Lydersen S, Hernes TN. Endovascular Image-Guided Navigation - Validation of Two Volume-Volume Registration Algorithms. Minim Invasive Ther Allied Technol. 2010 Nov 24.
3. **Manstad-Hulaas F**, Tangen GA, Gruionu LG, Aadahl P, Hernes TA. Three-Dimensional Endovascular Navigation with Electromagnetic Tracking – Ex Vivo and In Vivo Accuracy. J Endovasc Ther. 2011 Apr;18(2):230-40.
4. **Manstad-Hulaas F**, Tangen GA, Dahl T, Hernes TA, Aadahl P. Three-Dimensional Electromagnetic Navigation vs. Fluoroscopy for Endovascular Aneurysm Repair: A Prospective Feasibility Study In Patients. J Endovasc Ther. 2012 Feb;19(1):70-8.

4 LIST OF ABBREVIATIONS

3-D	Three-Dimensional
AAA	Abdominal Aortic Aneurysm
DICOM	Digital Imaging and Communications in Medicine
EM	Electromagnetic
EVAR	Endovascular Aortic Repair
EVNS	Endovascular Navigation System
FRE	Fiducial Registration Error
GPS	Global Positioning System
RMS	Root Mean Square
TAA	Thoracic Aortic Aneurysm
TAAA	Thoracoabdominal Aortic Aneurysm
TRE	Target Registration Error

5 INTRODUCTION

5.1 CLINICAL PERSPECTIVES

5.1.1 THE AORTIC ANEURYSM

An aortic aneurysm is a localized and permanent dilatation of the aorta, the diameter of which expands by more than 50% (1). Important risk factors for developing an aortic aneurysm include male gender, smoking history, older age, high blood pressure and history of aortic aneurysm in male first-degree relatives (1, 2). Depending on the location, an aortic aneurysm is usually classified as a thoracic aortic aneurysm (TAA), abdominal aortic aneurysm (AAA) or a thoracoabdominal aortic aneurysm (TAAA). Abdominal aneurysms are normally divided into juxta- or infrarenal aneurysms. Abdominal aortic aneurysms are by far the most common type, and approximately 15% of AAAs involve the juxtarenal aorta (3). As the maximum aneurysm diameter grows, the risk of rupture increases (2, 4). The rupture risk for large abdominal aortic aneurysms with diameters ≥5.5 cm is almost 10% annually in patients unsuited for treatment (4), whereas the rupture risk for AAAs <5.5 cm is ≤1% annually (5). As the risk of rupture increases, so does the relative benefit of aortic replacement. Aneurysm treatment is indicated at a diameter of ≥5.5 cm for both the thoracic and the abdominal aorta (2, 6-8) in patients with no genetic disorders (e.g., Marfan syndrome). Although physicians commonly use the absolute aortic diameter to predict aneurysm rupture, the aortic size index (ASI) may be more important. The ASI gives the relative aortic aneurysm size, as it is calculated by dividing the aortic diameter (in cm) by the body surface area (in m^2) (9).

The aortic wall consists of three layers: the intima, media and adventitia. Elastin, which is associated with smooth muscle cells and is predominantly localized in the media, is important for providing the aortic wall with its elastic properties. Collagen (types I and III), which is predominantly found in the adventitia, provides the aorta with tensile strength for structural integrity. Proteolytic enzymes, such as matrix metalloproteinases, from lymphomonocytic infiltrates and smooth muscle cells cause fragmentation and degradation of elastic and collagen fibers (10-15). The fragmentation of elastic fibers, decreased concentration of elastin and degradation of collagen are characteristic of aneurysmal tissue and play a critical role in the development and rupture of an aortic aneurysm (16-18).

Studies conducted before the 2000s indicated an increase in the prevalence of aortic aneurysms, but recent data suggest that this trend has reversed and that the prevalence of AAA is decreasing (19), as is the case with other cardiovascular diseases with similar risk factors. Abdominal aortic aneurysm is more common in men, with prevalence estimates ranging from 1.3-8.9% among men and 1.0-2.2% among women (20). Some patients may have vague symptoms, such as light abdominal or back pain, but most aortic aneurysms are asymptomatic until rupture. AAA rupture leads to death in approximately 65% of patients (21), and in developed countries, ruptured AAAs are responsible for 1.3% of all deaths among men aged 65-85 years. The preferred treatment to decrease rupture-related mortality is to exclude the aortic aneurysm from the arterial circulation. If one disregards the "wait and see approach", there are two treatment options: image-guided endovascular aortic repair (EVAR) and traditional open repair. The endovascular approach is discussed below.

5.1.2 HISTORICAL PERSPECTIVES ON ANGIOGRAPHY

Röntgen discovered X-rays in the late afternoon of 8 November 1895 in Würzburg, Germany, and received the first Nobel Prize in Physics in 1901. In 1896, the physicians Haschek and Lindenthal obtained the first angiogram of a hand by injecting a solution of bismuth, lead and barium salts into the brachial artery of a cadaver (22). In 1921, the French physicians Sicard and Forestier performed non-toxic intravenous injections of lipidiol (40% iodine in poppy oil) in humans, permitting radiographic visualization of the pulmonary arteries, and Osborne performed the first intra-arterial administration of iodine sodium at the Mayo Clinic in 1923 (23). After some initial difficulties, Egas Moniz performed the first successful, non-lethal cerebral angiography on 28 June 1927 by a direct carotid injection of 25% sodium iodide (24). In this early era of angiography, a peripheral injection of contrast medium did not facilitate the capture of acceptable radiographic images of arteries relatively far from the injection site. Werner Forssmann hypothesized that a flexible plastic tube could be inserted directly into the right atrium. In 1929, Forssmann became famous for an experiment in which he inserted a urethral catheter through his own antecubital vein into the right atrium and verified the catheter location on a plain radiograph (25). Later that year, Dos Santos, Lamas and Caldas introduced direct aortography by percutaneous, translumbar aortic needle puncture, but this technique caused a number of adverse effects, such as aortic dissection, rupture and thrombosis in visceral arteries (26).

Retrograde angiography, with a catheter inserted through the femoral artery in the groin, became popular after its introduction by Farinas in 1941, as physicians deemed this technique safer and the contrast medium could be injected at the desired site. Nevertheless, femoral access required a relatively time-consuming and occasionally

troublesome exposure of the artery and a large-bore needle to facilitate arterial access. This technique was sometimes complicated by hemorrhage. It was not until Seldinger introduced his technique in 1953 (27) that easy and safe access to the arterial system was achieved (Fig. 1). This technique "consists in the catheter being introduced on a flexible leader through the puncture hole after withdrawal of the puncture needle". With the Seldinger technique, angiography became relatively risk-free, leading to a marked increase in the number of interventional procedures performed. The same technique is used to facilitate endovascular interventions.

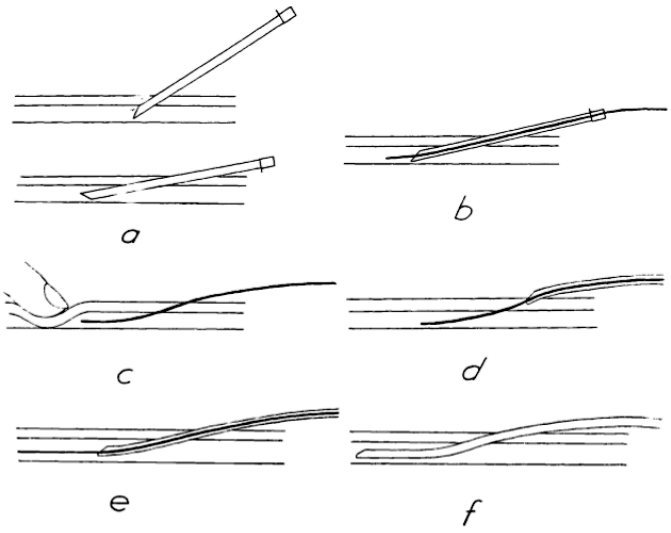

Figure 1. After arterial puncture (a) a guidewire is inserted (b) and the needle retracted (c). A catheter is pushed over the guidewire (d and e) before the wire is removed (f). Reprint with permission from the original article by Seldinger. ©2012 Royal Society of Medicine Press, UK.

Coltman invented the first X-ray image intensifier in 1948 (28), which made it possible to view X-ray images directly in daylight. The first commercial X-ray image intensifier appeared in the early 1950s and used mirror optics to present the image

(29). The image was viewed on a fluorescent screen (usually phosphor), which led to the naming of this technique as fluoroscopy. The introduction of fluoroscopy enabled the dynamic examination of the cardiovascular system following the intra-arterial injection of a contrast medium. In modern interventional radiology, flat-panel detectors with increased sensitivity to X-rays and better temporal resolution have replaced the image intensifiers. Digital video subtraction was developed in the 1970s and made it possible to subtract a pre-contrast X-ray image from a post-contrast X-ray image, presenting only the contrast loaded structures, i.e., the vasculature. The technique was initially applied using intravenously injected contrast medium, but in 1981, Crummy presented work using intra-arterial catheter-based injections with great success (30). Two important advantages of this technique, later known as digital subtraction angiography (DSA), were the reduced requirement for contrast medium and the ability to obtain a "road map". Today, fluoroscopy, angiography and digital subtraction angiography are cornerstones in endovascular intervention. In recent years, 3-dimensional DSA has also been gaining acceptance.

5.1.3 AN INTRODUCTION TO ENDOVASCULAR AORTIC REPAIR

In the 1950s the operative mortality rate for non-ruptured abdominal aortic aneurysm surgery was well above 20%, decreasing to 6.3% in the mid-1960s (31). Over the next 20 years, the operative mortality rate stayed relatively constant. Aiming to develop less invasive techniques, Volodos and his group performed the first minimally invasive implantation of an aortic endoprosthesis (32) in Kharkov, Soviet Union (today Ukraine), in 1986. Volodos et al. published their work in Russian, so their work never reached a larger audience. It was not until Parodi et al. published their paper, “Transfemoral intraluminal graft implantation for abdominal aortic aneurysms,” in 1991 that this technique became available to a broader medical

community (33). Since the work of Volodos and Parodi, there have been extensive developments in endovascular aortic repair. EVAR is routinely guided by fluoroscopy and DSA. The interventional radiologist or vascular surgeon normally inserts an aortic stent graft through the right (ipsilateral) femoral artery and the pelvic arteries, and into the aneurysmal aorta. The stent graft excludes the aneurysm sac from the circulation and reduces the risk of rupture. During endovascular repair of an AAA, the stent graft often must be extended into both iliac arteries to properly exclude the aneurysm sac from the circulation. In this case, an extension leg is inserted from the contralateral (usually the left) femoral artery into an opening in the main stent graft (Fig. 2). The EVAR Trial 1 showed reduced 30-day mortality in the EVAR group compared with the open-repair group (1.7% vs. 4.7%), although the long-term all-cause survival was similar between the two groups (34, 35). The improved 30-day survival may be attributed to the less invasive nature of the technique, and the 3% better aneurysm-related survival persisted throughout the 4-year follow-up period.

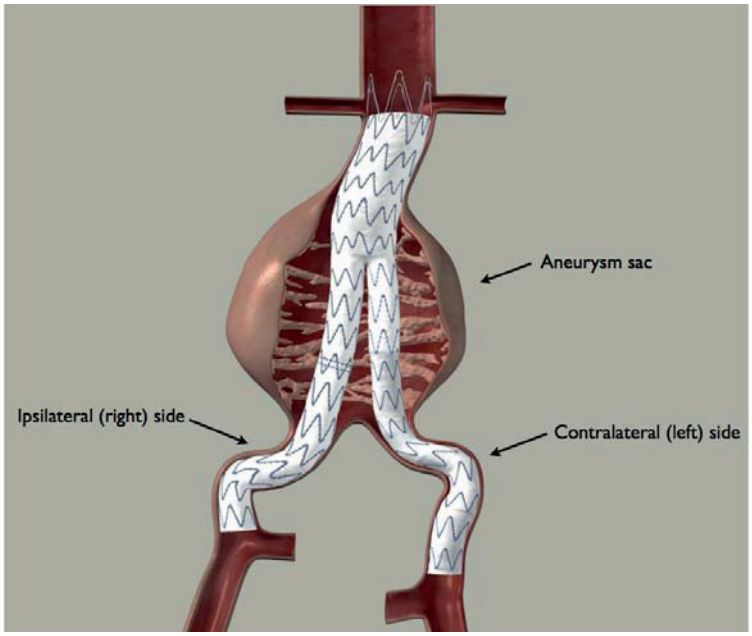

Figure 2. A bifurcated stent graft excluding an abdominal aortic aneurysm from the circulation. Photograph courtesy of Medtronic, Inc.

Although they are mandatory in all endovascular procedures, X-rays and contrast medium constitute some of the most important disadvantages of endovascular aortic repair, as they can cause skin erythema and contrast media-induced nephropathy (36, 37). Staff radiation exposure during endovascular procedures is low (38), but not negligible. It is also possible to treat complex aortic aneurysms, such as juxtarenal and thoracoabdominal aortic aneurysms, using endovascular techniques, but the stent graft is often patient-specific and may contain scallops, fenestrations or directional cuffs. Unfortunately, fluoroscopic and DSA images lack important spatial information about vessel anatomy, and such challenging procedures are time-consuming. Poor opacification in some regions of the aorta and the increased use of radiation and contrast medium constitute limitations in applying the endovascular approach to complex aneurysms (39).

5.2 NAVIGATION TECHNOLOGY

Computer-assisted surgery encompasses multiple methods in which pre- and/or intraoperative images are used in pre-surgical planning to improve surgical performance (e.g., to optimize tumor removal) and in image-guided procedures. A variety of imaging techniques can be used, including magnetic resonance imaging (MRI), computed tomography (including cone-beam computed tomography; CT), ultrasonography and other imaging modalities. In image-guided interventions, physicians use pre- and/or intraoperative image volumes to direct their use of instruments and tools during a variety of procedures. In recent years, navigation technology has undergone rapid developments in several different clinical areas. All

computer-assisted, image-guided interventions using navigation include a tracking system that reads the positions of all the devices and instruments inside the patients. In a navigation system, the instrument position displayed on the navigation image must correspond to the equivalent position in the patient. A registration must be performed to ensure correspondence between the patient anatomy and the navigation image before the procedure can begin. Tracking sensors can also register respiration or gross patient movement and thus provide an indication of whether the registration accuracy has deteriorated. The operator can see the position and orientation of the tracked instruments displayed on the registered image. The position of a tracked instrument is usually visualized on the navigation image as crosshairs or, alternatively, as a graphic icon of the instrument.

5.2.1 A BRIEF OVERVIEW OF TRACKING TECHNOLOGIES

The most common tracking technologies are explained below (40).

Spatial Linkage Systems

A mechanical linkage system is an assembly of several arms connected by joints, similar to a robotic arm. Neurosurgeons first used these systems for frameless stereotaxis in neurosurgery (41), but the best-known system today is most likely the Da Vinci Surgical System from Intuitive Surgical Inc. Spatial linkage systems are highly accurate, but tend to be relatively large and bulky.

Ultrasonic Tracking Systems

In ultrasonic tracking, the tracking system uses three microphones to triangulate high-frequency sounds from emitters attached to the instruments to calculate instrument positions. This technique is sensitive to noise, and obstacles between a sound emitter

and the microphones degrade the quality of the sound waves. So far, this technique has not gained traction in clinical medicine, but it has, for example, been used for the indoor positioning of mobile objects and people (42).

Optical Tracking Systems

Optical tracking technology utilizes cameras that detect light, either from active light-emitting diodes or passive reflecting trackers. In *active optical tracking*, diodes attached to instruments emit infrared light, whereas *passive optical systems* make use of trackers that reflect light. Both techniques use two or three cameras to detect the emitted/reflected light and thereby calculate the instrument's position. The diodes in active systems are either wired or use batteries, which makes them somewhat less suitable for use in medical interventions. Passive optical trackers normally use either high-contrast patterns of unique geometries that reflect available daylight or (at least) three spherical reflectors that reflects infrared light emitted from diodes around the camera lenses. Examples of common passive optical tracking systems include the Claron Micron Tracker (Claron Technology Inc., Ontario, Canada) and the Polaris System (Northern Digital Inc., Ontario, Canada; Fig. 3A). Optical tracking is well proven, with a volumetric accuracy in the range of 0.25 mm (43); however, optical tracking has three main disadvantages. First, it requires a direct line of sight, which means that tracking is instantly interrupted if an object passes between the cameras and trackers. Furthermore, the accuracy depends on the distance between the spherical reflectors; thus, the trackers tend to be large. The trackers are normally attached to the proximal end of an instrument (Fig. 3B); therefore, the instruments must be rigid to calculate the position of the instrument tip. These factors make optical tracking less suitable for use in endovascular procedures.

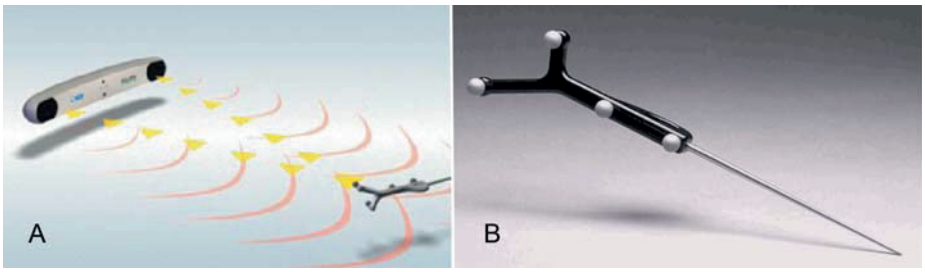

Figure 3. ***A*** *The principle behind optical tracking is the detection of objects that reflect light from markers arranged in a known geometry. When spherical reflectors are used for passive tracking, a cluster of at least three reflectors is needed, as illustrated in this figure. If high-contrast printed patterns of unique geometry are used, two reflectors are sufficient.* ***B*** *A passive optical tracker with four spherical markers reflecting infrared light is mounted on a probe. The instrument must be rigid, and a direct line between the camera lenses and the spherical markers is necessary to obtain the instrument position. Courtesy of Northern Digital Inc.*

Electromagnetic Tracking Systems

A fluctuating electromagnetic (EM) field will induce a current in any coils located within this field. This basic principle underlies positioning in electromagnetic tracking. A field generator placed near an object or patient produces an electromagnetic field, and the position of any coils, i.e., position sensors, within this field can be calculated based on the current induced in the coils. The physical volume within which position sensors are tracked is normally referred to as the *tracking space*. The position sensors are cylindrical, normally 0.5-1 mm in diameter and 5-10 mm in length (Fig. 4A). The small size of the position sensors, which makes them suitable for integration into various instruments, and the absence of a line-of-sight constraint make them ideal for tracking instruments and devices inside a patient during endovascular procedures. The most common stand-alone systems for

electromagnetic tracking are the Aurora (Northern Digital Inc.) and the 3D Guidance (Ascension Technology Corp., Milton VT, USA) systems (Fig. 4B). Their suitability for use in the interventional radiology suite has previously been thoroughly assessed (44).

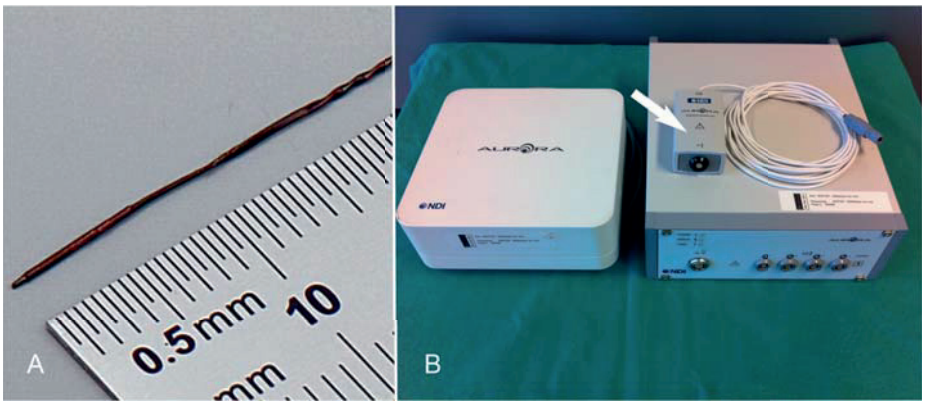

Figure 4. ***A*** *This figure shows a position sensor measuring 0.5 x 8mm. Photograph courtesy of Northern Digital Inc.* ***B*** *An electromagnetic tracking system consists of a field generator, one or multiple sensor interface units (white arrow), and a control unit.*

Despite the suitability of electromagnetic tracking systems for use in minimally invasive interventions, it is important to be aware of possible interference with positional accuracy. There is no uniform or standardized categorization of electromagnetic tracking system errors, but one approach that is gaining acceptance is to divide the errors into static and dynamic errors (45, 46). Static errors can be further subdivided into jitter errors and static distortions, which are typically caused by ferromagnetic instruments and electronic devices. Jitter errors are in the sub-millimeter range, 0.15 ± 0.12 mm for the 3D Guidance system from Ascension (46), and static distortions depend on the size and proximity of the ferromagnetic object. Dynamic errors are subdivided into sensor-velocity errors and dynamic distortions. Velocity errors occur when an instrument/sensor moves quickly and depend on the

velocity/acceleration of the sensor, whereas dynamic distortions arise when ferromagnetic or electronic devices enter the electromagnetic tracking volume during a run. Recent hardware and software improvements have reduced the influence of static errors.

5.2.2 NAVIGATION SYSTEM WITH ELECTROMAGNETIC TRACKING

Most navigation systems based on electromagnetic tracking share some common elements, such as a computer workstation, one or more navigation screens, navigation software, an electromagnetic generator, position sensors with sensor-interface units and a control unit. The latter three components constitute an electromagnetic tracking system as described above, and commercially available systems, such as the 3D Guidance and Aurora systems, are frequently used.

5.2.3 NAVIGATION SYSTEM WITH EM TRACKING IN MEDICAL PROCEDURES

Navigation systems based on 3-D images and electromagnetically tracked instruments and tools have been tested in pilot studies and used in clinical practice in a wide range of applications, including transbronchial biopsies, laparoscopic ultrasound, radiofrequency ablation, neuronavigation, orthopedic surgery and cardiac ablation (47-55). Abi-Jaoudeh et al. demonstrated the feasibility of inserting a thoracic stent graft using a navigation system based on 3-D images and electromagnetic tracking in an animal trial (56); however, in general, navigation systems are rarely used for endovascular procedures. Some manufacturers have integrated the capability of 3-D visualization during endovascular procedures into the angiography equipment, as in the syngo iPilot system from Siemens. This technique may enhance spatial information and reduce the use of contrast medium, but it does not enable endovascular navigation of catheters and guidewires. An endovascular navigation

system (EVNS) based on the electromagnetic tracking of tools, such as guidewires and catheters, and 3-D images may improve established endovascular repair and prove helpful in complex procedures.

6 AIMS OF THE RESEARCH

6.1 BACKGROUND AND MOTIVATION

For more than two decades, conventional fluoroscopy and angiography have constituted the sole navigational aids used in endovascular aortic repair. To achieve correct alignment of a stent graft without compromising visceral arteries, adequate visualization is of the utmost importance. For most EVARs of simpler thoracic and abdominal aneurysms, fluoroscopy and angiography are sufficient. For more complicated and challenging repairs (most thoracoabdominal and juxtarenal aneurysms), stent grafts with scallops, fenestrations and directional cuffs are used (57, 58). Due to the anatomic complexity and need for cannulation of visceral arteries, traditional fluoroscopy and angiography techniques can prove insufficient.

Patients undergoing all types of EVARs are at risk for contrast-induced nephropathy (CIN). Patients with pre-existing renal impairment and diabetes are particularly at risk (59), and the risk is likely to increase in more complicated procedures (60). Radiation is a necessity during EVAR, but should be minimized; however, the radiation applied during EVAR can become substantial and is expected to increase during complicated procedures (36, 61). Navigation systems based on 3-D images and EM-tracking are used in a number of surgical specialties (47-55) to provide the operators with more anatomic information and to make intraoperative navigation safer and more accurate. It is likely that an EVNS can provide the same benefits in simpler as well as complex EVAR procedures.

Before any navigation can take place, the navigation images must be registered to the patient (or object) in whom navigation is performed. It is relatively simple to register a 3-D image acquired with a cone-beam CT in the angiography suite to a patient.

Such image volumes are thus well suited for intraoperative navigation; however, the image volume created from a cone-beam CT depends on the size of the flat-panel detector and may not always cover the complete anatomy of interest. One possible solution to this problem is to merge (co-register) a preoperative CT image covering the area of interest with the intraoperatively acquired cone-beam CT image. The navigation software must have the ability to register and use multiple, overlaid image volumes of a patient for navigation; a successful volume-to-volume registration depends on accurate and reliable registration algorithms.

6.2 STUDY OBJECTIVES

The overall aim of this thesis was to test the usability of navigation technology for endovascular aortic repair and to demonstrate its accuracy in clinical application.

STUDY 1

The main purpose of this study was to evaluate the feasibility of inserting a stent graft with one side branch in a phantom AAA using an endovascular navigation system. Furthermore, we investigated the user-friendliness of the navigation system and tested whether navigation technology could reduce radiation exposure, shorten the procedure time and simplify the insertion of the guidewire into a renal artery on a phantom.

STUDY 2

The aim of this study was to validate and quantify the accuracy of volume-to-volume registration algorithms. Two algorithms were studied using CT images from patients undergoing EVAR. One algorithm was developed especially for endovascular use, and the other was developed for the general registration of CT images.

STUDY 3

The aim of this study was to quantify the clinical application accuracy of an endovascular navigation system. The accuracy was evaluated first *ex vivo* in a phantom and then *in vivo* in a porcine model. The study was conducted under regular surgical conditions in the angiography suite at St Olavs Hospital, Trondheim.

STUDY 4

The purpose of this open and randomized patient study was to investigate the usability of an endovascular navigation system with electromagnetically tracked catheters as an extra visualization tool during EVAR.

7 MATERIALS AND METHODS

This and the following chapters will provide a detailed description of the navigation system used in the studies that form the basis of this thesis.

7.1 ELECTROMAGNETIC TRACKING

The commercially available electromagnetic tracking system Aurora (Northern Digital Inc., Waterloo, Canada) was used to conduct the practical work for this thesis. A system control unit, a field generator, and one or more position sensors and sensor-interface units constituted the electromagnetic tracking system. The field generator and sensor-interface units were connected to the control unit, which in turn was connected to a computer workstation. The field generator produced an electromagnetic field of approximately 0.5 x 0.5 x 0.5 m. A current was induced in all position sensors located within the electromagnetic field. This current was related to the position and orientation of the sensor. Position refers to the translation in three perpendicular axes (x, y, and z), and orientation refers to the rotation (pitch, yaw and roll), for a total of six degrees of freedom (DoF). A 6-DoF sensor has the ability to provide data for all six degrees of freedom, while a 5-DoF sensor lacks information about roll. The applied 5-DoF sensors measured 0.8 x 11 mm and 0.5 x 8 mm, and the 6-DoF sensors measured 1.8 x 9 mm. The positional accuracy of the Aurora system, according to the manufacturer (Northern Digital Inc.), was 0.9-1.3 mm (root mean square, RMS) for the 5-DoF sensors used in Study 1. When Study 3 and 4 took place the positional accuracy of the Aurora system was improved due to technological refinements with the following values: RMS = 0.70 mm (95% CI = 1.40 mm) for 5-DoF sensors, and RMS = 0.48 mm (95% CI = 0.88 mm) for 6-DoF sensors (62).

Although the 6-DoF sensors were larger than the 5-DoF sensors, they achieved higher accuracy.

7.2 NAVIGATION SOFTWARE (CustusX)

This project used a prototype navigation software for 3-D navigation, namely the CustusX navigation platform (SINTEF, Dept. of Medical Technology, Trondheim, Norway), an image-guided therapy system developed for use in minimally invasive procedures. CustusX evolved within the National Centre of Competence in Ultrasound and Image-Guided Therapy, which was founded in 1995 by the cooperating partners SINTEF, St Olavs Hospital and the Norwegian University of Science and Technology. Fellow researchers developed the CustusX navigation platform to support research studies in the operating room (OR), especially in neurosurgery, vascular surgery and laparoscopic surgery. Research has since extended into new clinical areas such as spine surgery, bronchoscopy and lung biopsy. Physicians at St Olavs Hospital use this navigation system to guide minimally invasive procedures by integrating multimodal medical image information, and presenting intuitive visualizations to the operator that are augmented with real-time positioning of the tools. Both optical and electromagnetic tracking systems are supported, and the complete system is mounted on a trolley for easy transport and integration into the OR workflow (Fig. 5).

Figure 5. The in-house navigation system consists of a computer workstation on which the navigation software is installed, a navigation screen and a control unit. The navigation image can also be streamed to a larger, roof-mounted screen next to the operator in the operating room.

Software developers designed the system for cross-platform operation (to run on an off-the-shelf PC, Linux or Macintosh computer workstation) and based the software on the open-source libraries Qt (www.qt.nokia.com), Visualization Toolkit (www.vtk.org), Insight Toolkit (www.itk.org) and Image-Guided Surgery Toolkit (www.igstk.org).

The operator can import medical image data in DICOM (Digital Imaging and Communications in Medicine) format with pre-processed segmented models (e.g., segmented blood vessels, tumors, and bone anatomy). CT volumes, 3-D ultrasound and MRI data can be stored in DICOM format and be imported into CustusX. The navigation software registers image data to the patient via optically or electromagnetically tracked fiducial markers that are also visible in the images. After registration the image data can be visualized as 3-D computer graphics or as orthogonal images that provide the position and orientation of the tracked instrument, providing visual guidance during the procedure (Fig. 6). There is also an "any-plane" option, in which a 2-D CT image (similar to the orthogonal slices and also containing the position of the tracked instrument) can be visualized together with the 3-D image in any desired plane. The navigation system can merge and enable visualization of real-time (streamed) fluoroscopy, ultrasound and endoscopic video as well as the preoperative images. Images acquired intraoperatively can be used to update the navigation display with, for example, changes and anatomical shifts, as they occur during the procedure.

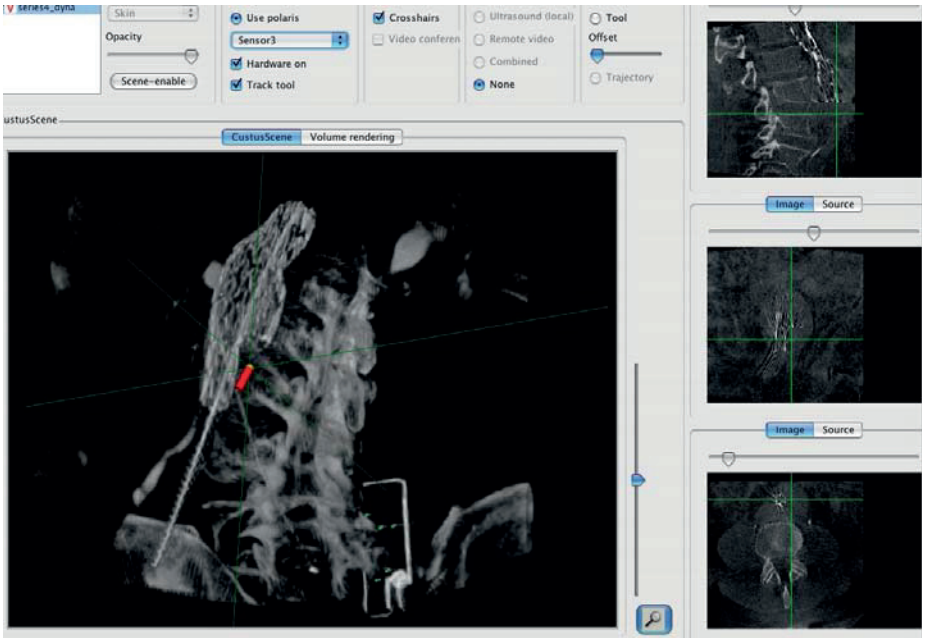

Figure 6. Image data is displayed as a 3-D image with (as in this figure) or without three orthogonal slices on the left side. All position sensors (or instruments) can be visualized in the 3-D image. The orthogonal slices can provide position data for only one of the position sensors, but the operator can choose which sensor to track.

The advantage of using a prototype navigation system rather than a commercial alternative is that we have full access to all internal data (e.g., images and tool position data) generated during the procedure. It is thus easier to include and take advantage of new developments in the open source library base. Having full access to the code base also makes development and inclusion of new functionality relatively easy. This access also makes it possible to adapt the system to new clinical procedures and manufacture new, tracked instruments according to clinical requirements; however, all of these developments require that a software team be involved in the research project.

7.3 IMAGE ACQUISITION AND REGISTRATION

All images used for navigation during this project were acquired with a roof-mounted cone-beam CT (Siemens AXIOM Artis dTA®, Siemens AG Healthcare Section, Forchheim, Germany), and all image volumes contained a reference plate (fiducial). The reference plate was attached to the object or the patient's back, and contained seven radio-opaque markers and two 5-DoF position sensors (Fig. 7A). As the configuration of the radio-opaque markers relative to the two 5-DoF position sensors was known, the position of the radio-opaque markers in the tracking space could be calculated and visualized on the navigation screen as seven green dots. After the CT image containing the reference plate was imported into the navigation software, the CT image was manually registered to the tracking space by overlaying the radio-opaque markers on the CT image with the corresponding green dots in the tracking space (Fig. 7B).

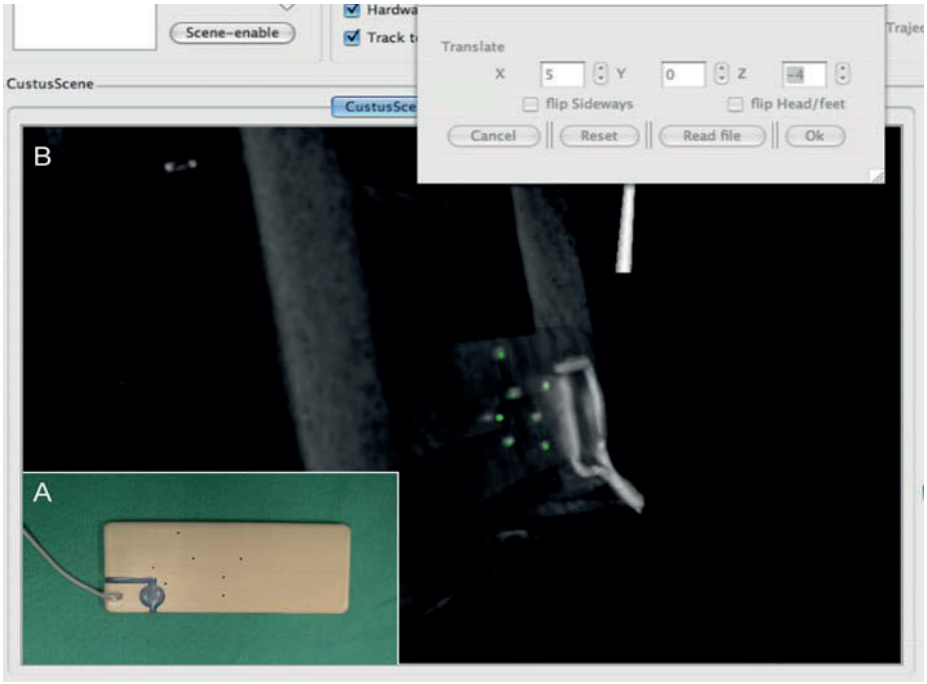

Figure 7. ***A*** *The reference plate contained 7 radio-opaque metal spheres. It was attached to the patients, animals, and models and was always included in the acquired image volume.* ***B*** *A CT image is manually registered to a patient. During manual registration, the CT image was moved within the electromagnetic tracking space until the spheres were overlaid on the corresponding green dots.*

7.4 STATISTICS

In the studies included in this thesis, we used descriptive statistics, univariate analysis, linear mixed models and the Mann-Whitney U test. All statistics were computed with SPSS 13.0 or 18.0 (SPSS, Chicago, IL, USA)

8 SUMMARY OF STUDIES AND MAIN FINDINGS

PAPER 1

The study presented in Paper 1 evaluated the usability of a custom-made, side-branched stent graft that was inserted into an artificial abdominal aortic aneurysm using the endovascular navigation system. In the control trials, the procedure was executed with fluoroscopy alone. We also investigated whether the use of the navigation system reduced radiation exposure and operation time, and we explored the user-friendliness of the navigation system. All participating physicians accomplished invariably successful stent graft insertion, including control trials. There was no significant difference in the overall procedure time; however, a learning effect was observed for the navigation system, as procedure time declined with the number of insertions performed. A significant reduction in radiation exposure was observed as the overall procedure time declined. The navigation system was considered user-friendly.

PAPER 2

Two algorithms for image-to-image registration, developed by Siemens (Siemens AG Healthcare Section, Forcheim, Germany) and CAMP (Chair for Computer Aided Medical procedures, Technical University, Munich, Germany), were tested for registration accuracy. Five anatomical landmarks in the registered image volumes were used for accuracy evaluation. The mean RMS ± SD was 5.05 ± 4.74 mm for the Siemens algorithm and 4.02 ± 1.52 mm for the CAMP algorithm. The median RMS values were 3.58 mm and 3.68 mm for the Siemens and CAMP algorithms

respectively. Both algorithms were deemed suitable for image-to-image registration, but the CAMP algorithm was slightly more accurate and robust.

PAPER 3

The clinical application accuracy of the endovascular navigation system was studied both *ex vivo* and *in vivo*. The *ex vivo* navigation accuracy was calculated from 57 measurements. The mean distance between the tracked and actual needle tip positions was 1.28 ± 0.53 mm, and the median distance was 1.23 mm. In the *in vivo* sub-study, 24 guidewire tip positions were registered. The mean and median distances between the tracked and actual guidewire tip positions were 4.18 ± 1.76 mm and 3.99 mm respectively. Of the measured distances, 90% were ≤ 5.73 mm.

PAPER 4

In Paper 4, the contralateral cuff of a bifurcated stent graft was catheterized using the endovascular navigation system. Control trials were performed with fluoroscopy alone. Catheterizations of the contralateral cuff with an electromagnetically tracked catheter were successful in 6 of 7 patients (86%). In the control group, placement of a catheter within the main stent graft was successful in 8 of 10 patients (80%). A maximum of 8 attempts were needed to insert the guidewire correctly in the intervention group, compared with a maximum of 33 attempts in the control group. Similar contrast amounts and procedure times were found between the intervention and control groups. However, the total radiation dose was higher in the intervention group ($p=0.043$).

9 DISCUSSION AND FUTURE PERSPECTIVES

From its humble beginnings in the early 1990s to the present, endovascular aortic repair has undergone dramatic developments. The most influential changes over this period include improvements in stent grafts and delivery techniques. Examples of improvements include better graft material, the introduction of nitinol stents and better anchoring of the stent struts. More versatile introducer sheaths with lower profiles have also made EVAR simpler and more readily applicable. However, the guiding techniques used to insert and deploy a stent graft are still confined to fluoroscopy and digital subtraction angiography, techniques that have changed relatively little over time.

EVAR has become an established and increasingly popular treatment, and the percentage of AAAs deemed suitable for endovascular treatment has grown in recent years, mostly as a result of the improvements described above. Certain criteria or systems to score the anatomical characteristics of aneurysms can be used to assess whether a patient is eligible for EVAR (2, 63), and the manufacturing instructions of commercially available stent grafts may constitute further limitations. Endovascular techniques are usually confined to repairs of the descending and infrarenal aorta, although traditional open surgery of thoracoabdominal aortic aneurysms has been, and still is, encumbered with relatively high short- and long-term mortality and morbidity rates (64, 65). Endovascular techniques should also be applicable to the repair of complex aneurysms.

The first small studies and case reports on the endovascular repair of complicated thoracoabdominal aneurysms with fenestrated stent grafts were performed in the early 2000s (66, 67). In a multicenter trial by Greenberg et al. (68), the intermediate result

after endovascular repair of juxtarenal aneurysms was promising, with no short or mid-term deaths related to the AAA repair, but the procedure time was a prolonged (median 234 min). Furthermore, the catheterization of aortic branches through stent graft fenestrations and directional cuffs can present a major challenge during complex EVAR. Although EVAR has a lower odds ratio for developing contrast-induced nephropathy (CIN) compared with open AAA repair (69), this risk is far from negligible. EVAR patients are older and are more likely to have chronic renal failure and diabetes, which increase the risk of CIN (37, 70). This point brings us to the disadvantages of interventional radiology, which are the use of ionizing radiation and nephrotoxic contrast medium. The present work was thus conducted to address these disadvantages. Endovascular navigation systems may improve the visualization of vascular anatomy and endovascular navigation in EVAR, especially in challenging procedures with difficult catheterizations in which detailed spatial information is crucial. Furthermore, these systems may reduce radiation exposure, contrast medium required, and operation time in both time-consuming and standard procedures, thus making the procedures more readily applicable. This thesis was developed in an attempt to clarify these possibilities by assessing the usability and the clinical application accuracy of our in-house endovascular navigation system, CustusX. Trials have progressed gradually from *in vitro* tests on phantoms to *in vivo* studies in animals and humans.

9.1 ENDOVASCULAR NAVIGATION IN STENT GRAFT IMPLANTATION

Our main purpose in the study described in **Paper 1** was to implant a side-branched stent graft in an AAA phantom using the navigation system CustusX in conjunction with fluoroscopy, as well as to compare these results with stent graft insertions guided by fluoroscopy only. The study demonstrated the usability of this navigation system,

and we achieved a significant reduction in radiation when the navigation system was used. However, when the radiation doses were calculated, the preoperative cone-beam CT of the phantom was left out. Whether this was a correct decision is open to debate, but a study by Eide et al. (71) showed that the dose-area product and effective dose added by the same cone-beam CT as that used in our studies are relatively modest. In addition, the cone-beam CT in the study by Eide et al. was performed during contrast injection, increasing exposure to radiation during image acquisition. In this study, as in a clinical setting, we did not use contrast medium, which would further reduce the radiation from the intraoperative cone-beam CT.

After an initial learning phase, both the time needed for guidewire placement in the renal artery and the procedure time were shorter when using the navigation system compared with the fluoroscopy only, but the differences were not statistically significant. This type II error is one of the weaknesses of this study and could most likely be avoided by increasing the number of trials. On the other hand, the results are encouraging with regard to the user-friendliness of the navigation system, as all participants quickly adapted to the new technique. This result suggests that the training of medical personnel and clinical implementation of navigation technology can be conducted relatively easily.

9.2 REGISTRATION OF IMAGE VOLUMES

In **Paper 2**, we tested the accuracy of two algorithms that were developed to register image volumes for use in endovascular navigation. The study was intended to test the algorithms by registering preoperative CT images to intraoperative CT images, but the intraoperative images were acquired after stent graft implantation. Because the postoperative CT images also contained the implanted stent graft, we decided to register the intraoperative to postoperative images, as they were more similar.

However, the article could have elaborated more on why registering pre- and intraoperative images can be beneficial in endovascular navigation. Preoperative CT images can be used for navigation without acquiring intraoperative CT images, but only under certain conditions. The most common technique for the direct use of a preoperative CT image for navigational purposes is to attach fiducial markers to the patient's skin covering the volume of interest, prior to image acquisition. Then, the corresponding points (fiducial markers) in the image volume and tracking space can be registered to each other (image-to-patient registration). Unfortunately, the skin is a relatively soft tissue, and shifts/skin displacements can occur between the image acquisition and the image-to-patient registration in the operating room. For preoperative magnetic resonance imaging (MRI), Mitsui et al. demonstrated a skin shift of 5.34 (± 2.65) mm for fiducial markers attached to the head with a navigation accuracy of 4.06 (± 2.25) mm (72), however, for intraoperatively acquired MRI, the navigation accuracy was 2.51 (± 1.32) mm. For fiducial markers attached to the abdomen, one has to expect further deterioration of navigation accuracy, especially in obese patients. According to Fitzpatrick et al. (73), correct placement of the fiducial markers is crucial to target registration, which refers to the correspondence of the displayed position of an instrument on the navigation image with the equivalent anatomical position inside the patient. The uncertainty associated with the image-to-patient registration of a preoperative CT image based on fiducial markers was the motivation for using an intraoperatively acquired CT image for navigation. In cases in which physicians must work with instruments outside the intraoperatively acquired CT volume, the localization of the instruments can be visualized in the larger preoperative CT image registered to the smaller intraoperative CT image. Furthermore, in a clinical setting, the preoperative CT image is usually acquired

weeks before the endovascular procedure, which practically precludes the use of fiducial markers for image-to-patient registration.

9.3 ENDOVASCULAR NAVIGATION SYSTEM ACCURACY

During the *in vivo* accuracy testing of the endovascular navigation system reported in **Paper 3**, a reference plate was attached to the backs of the swine at the point where the renal arteries were assumed to branch off. If the placement of the reference plate was sub-optimal, the acquired CT image would exclude some of the visceral arteries. Because the ostia of the visceral arteries were targets for navigation, alternative targets had to be found. It would have been better to start with regular angiography to locate the branching visceral arteries and then seek out the best position for the reference plate.

For all navigation systems used during medical procedures, it is important to demonstrate a satisfactory degree of accuracy in clinical applications. The instruments or tools being navigated should be, with a satisfactory degree of accuracy, located at the physical location corresponding to the position in the navigation image. The operator must assess the degree of accuracy necessary to perform a procedure, but to do this the operator must be familiar with this term and understand its meaning. Furthermore, "accuracy" must be distinguished from "precision". When an instrument is navigated repeatedly to the same target, the actual positions will be scattered randomly around the target. The dispersion of the actual positions corresponds to the reproducibility or precision, while the mean distance to the target corresponds to the accuracy. The randomly scattered positions are also referred to as target registration errors (TREs), and are normally distributed around the target. If a navigation system can guide an instrument to the same position (good precision), but the instrument is always outside the target (poor accuracy), the error is systematic (Fig. 8). As also

discussed in Paper 3, it is of the utmost importance that the operator does not confuse the fiducial registration error (FRE) with the TRE, as these are uncorrelated (74). Navigation systems usually provide the FRE as an indicator of the image-to-patient registration accuracy. Confusion may lead the operator to believe that the targeted position of an instrument is adequate, even when this may not be the case.

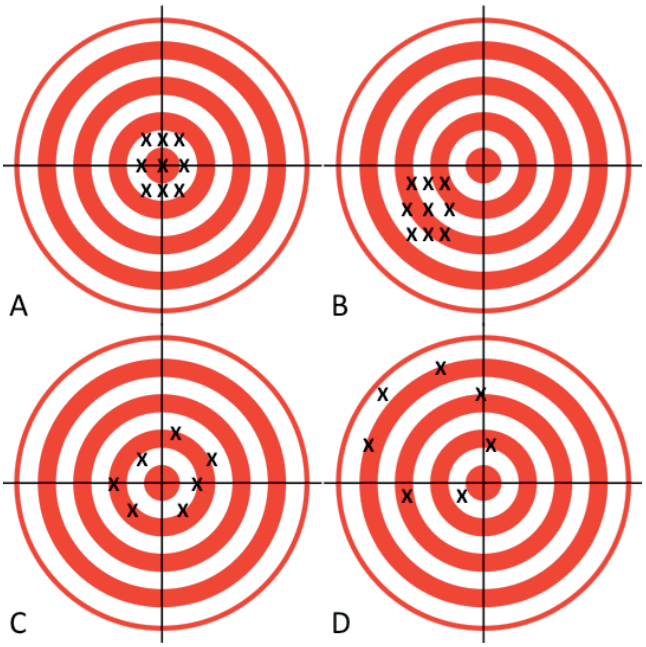

Figure 8. ***A*** *High accuracy, high precision.* ***B*** *Poor accuracy, high precision (systematic error).* ***C*** *High accuracy, poor precision.* ***D*** *Poor accuracy, poor precision.*

To facilitate catheter navigation, a small 5-DoF sensor was embedded in the catheter tip, as described in the paper. Although 6-DoF sensors provide better position accuracy, their larger diameter rendered them unsuitable for integration into the catheters; however, since this study was conducted, smaller 6-DoF sensors suitable for integration have been developed. In addition to the other factors discussed in the paper, the use of 6-DoF sensors in the catheters would further improve the accuracy of the navigation system in clinical applications.

9.4 ENDOVASCULAR NAVIGATION IN PATIENTS

In recent years, several research institutions have conducted trials to assess the usability of electromagnetic navigation in endovascular procedures. With the exception of two experimental studies conducted in swine by Wood et al. (75) and Abi-Jaoudeh et al. (56), all studies have been performed *ex vivo* using various aortic phantoms. Thorough *ex vivo* tests of new technology are necessary, but when the results of these validity tests are satisfactory, it is necessary to explore the technology through experimental trials in animal models and patients. In addition, manufacturers have improved and refined the electromagnetic tracking technology in recent years. Endovascular navigation based on electromagnetic tracking should thus be ready for clinical trials. Despite the low number of included patients in this thesis, we demonstrated the first successful feasibility tests in patients in **Paper 4**.

One intended benefit of using the EVNS during EVAR was to reduce radiation exposure; however, during the feasibility tests in Study 4, we were unable to reduce the radiation in patients undergoing EVAR with the navigation technology. Although an additional, intraoperative cone-beam CT image was needed to facilitate the 3-D navigation, the lack of a reduction in radiation exposure is most likely due to random variability and the small number of included patients. In a study including 20 patients, Eide et al. (71) showed that the mean radiation dose (dose-area product) added by cone-beam CT scanning, identical to that used in **Paper 4**, was only 3027 μGym^2. These findings support the assumption that the lack of a reduction in radiation was caused by random variability and a low number of patients.

9.5 FUTURE PERSPECTIVES

Research on endovascular navigation will remain a research priority at St Olavs Hospital, SINTEF Dept. of Medical Technology and the Dept. of Circulation and Medical Imaging, NTNU. This thesis has not only brought new insight into endovascular navigation, but it also indicates areas in need of improvement. During the writing of this thesis, we encountered a problem that is common to research in which new technologies are developed and tested, namely a lack of integration with existing, commercially available equipment. The angiography suite became crowded with additional equipment used in the experimental setup, hampering a good workflow and which, in turn, may have influenced the results. A refined and user-friendly integration of the endovascular navigation system and tracked instruments with the conventional angiography equipment would significantly improve workflow. Recently, Siemens Healthcare could offer Artis zee™ angiography systems with an integrated electromagnetic tracking system that localizes the catheter in use and projects its position on a previously acquired fluoroscopy image. Currently, this navigation system is available only with a 20x20 cm flat panel detector for cardiac interventions. Other suppliers of angiography systems would most likely follow suit, resulting in the extended applicability of this system beyond cardiac procedures. During conventional endovascular aortic repair, the physician can relatively easily and quickly switch between different catheters. It is somewhat more cumbersome to change an electromagnetically tracked catheter, and we experienced reduced catheter maneuverability during the *in vivo* tests. Both factors reduce the usability of an endovascular navigation system. In future studies, therefore, we will manufacture and test tracked, steerable and agile catheters that limit the need to switch between catheters. Procedures using electromagnetically tracked guidewires should be

especially affected by such a development, because to facilitate catheter exchange the tracked guidewire must be retracted. With the combination of tracked, steerable catheters and tracked guidewires, we should be able to perform large portions of the endovascular navigation and cannulations without radiation and contrast medium.

As a shift from open surgery to endovascular repair of juxtarenal and thoracoabdominal aortic aneurysms will inevitably occur, questions related to total costs and the durability of stent grafts will need further clarification. For infrarenal aortic aneurysms, the UK EVAR program showed that EVAR, in the long term, is more expensive than open surgery (76). Although there may be an initial decrease in costs, mainly due to reduced perioperative morbidity and shorter hospital stays, it is very likely that the overall, long-term costs for complex aneurysms will be higher for endovascular repair than for open surgery. With regard to durability, a recent study by Reilly et al. (77) showed acceptable intermediate durability of complex aortic aneurysms after EVAR in 81 patients, however, until larger patient populations with longer follow-ups are studied, this question will remain incompletely answered.

10 CONCLUSIONS

This thesis demonstrates the potential of an endovascular navigation system to improve guidance and reduce the use of radiation and contrast medium in endovascular aortic repair. An endovascular navigation system can most likely facilitate the repair of aortic aneurysms, including more complex cases, however, it is necessary to integrate navigation technology into existing commercial angiographic equipment to simplify the workflow. In addition, larger clinical trials should be conducted to study the clinical implications of such navigation systems.

11 REFERENCES

1. Johnston KW, Rutherford RB, Tilson MD, Shah DM, Hollier L, Stanley JC. Suggested standards for reporting on arterial aneurysms. Subcommittee on Reporting Standards for Arterial Aneurysms, Ad Hoc Committee on Reporting Standards, Society for Vascular Surgery and North American Chapter, International Society for Cardiovascular Surgery. J Vasc Surg. 1991 Mar;13(3):452-8.
2. Moll FL, Powell JT, Fraedrich G, Verzini F, Haulon S, Waltham M, et al. Management of abdominal aortic aneurysms clinical practice guidelines of the European society for vascular surgery. European Journal of Vascular and Endovascular Surgery. 2011 Jan;41 Suppl 1(1):S1-S58.
3. Taylor SM, Mills JL, Fujitani RM. The juxtarenal abdominal aortic aneurysm. A more common problem than previously realized? Arch Surg. 1994 Jul;129(7):734-7.
4. Lederle FA, Johnson GR, Wilson SE, Ballard DJ, Jordan WD, Jr., Blebea J, et al. Rupture rate of large abdominal aortic aneurysms in patients refusing or unfit for elective repair. Jama. 2002 Jun 12;287(22):2968-72.
5. Wilt TJ, Lederle FA, Macdonald R, Jonk YC, Rector TS, Kane RL. Comparison of endovascular and open surgical repairs for abdominal aortic aneurysm. Evid Rep Technol Assess (Full Rep). 2006 Aug;144(144):1-113.
6. Brewster DC, Cronenwett JL, Hallett JW, Jr., Johnston KW, Krupski WC, Matsumura JS. Guidelines for the treatment of abdominal aortic aneurysms. Report of a subcommittee of the Joint Council of the American Association for Vascular Surgery and Society for Vascular Surgery. J Vasc Surg. 2003 May;37(5):1106-17.
7. Hiratzka LF, Bakris GL, Beckman JA, Bersin RM, Carr VF, Casey DE, Jr., et al. 2010 ACCF/AHA/AATS/ACR/ASA/SCA/SCAI/SIR/STS/SVM guidelines for the diagnosis and management of patients with Thoracic Aortic Disease: a report of the American College of Cardiology Foundation/American Heart Association Task Force on Practice Guidelines, American Association for Thoracic Surgery, American College of Radiology, American Stroke Association, Society of Cardiovascular Anesthesiologists, Society for Cardiovascular Angiography and Interventions, Society of Interventional Radiology, Society of Thoracic Surgeons, and Society for Vascular Medicine. Circulation. 2010 Apr 6;121(13):e266-369.
8. Lederle FA, Wilson SE, Johnson GR, Reinke DB, Littooy FN, Acher CW, et al. Immediate repair compared with surveillance of small abdominal aortic aneurysms. N Engl J Med. 2002 May 9;346(19):1437-44.
9. Davies RR, Gallo A, Coady MA, Tellides G, Botta DM, Burke B, et al. Novel measurement of relative aortic size predicts rupture of thoracic aortic aneurysms. Annals of Thoracic Surgery. 2006 Jan;81(1):169-77.
10. Carrell TW, Burnand KG, Wells GM, Clements JM, Smith A. Stromelysin-1 (matrix metalloproteinase-3) and tissue inhibitor of metalloproteinase-3 are overexpressed in the wall of abdominal aortic aneurysms. Circulation. 2002 Jan 29;105(4):477-82.

11. Longo GM, Xiong W, Greiner TC, Zhao Y, Fiotti N, Baxter BT. Matrix metalloproteinases 2 and 9 work in concert to produce aortic aneurysms. J Clin Invest. 2002 Sep;110(5):625-32.
12. Nollendorfs A, Greiner TC, Nagase H, Baxter BT. The expression and localization of membrane type-1 matrix metalloproteinase in human abdominal aortic aneurysms. J Vasc Surg. 2001 Aug;34(2):316-22.
13. Sakalihasan N, Delvenne P, Nusgens BV, Limet R, Lapiere CM. Activated forms of MMP2 and MMP9 in abdominal aortic aneurysms. J Vasc Surg. 1996 Jul;24(1):127-33.
14. Thompson RW, Parks WC. Role of matrix metalloproteinases in abdominal aortic aneurysms. Ann N Y Acad Sci. 1996 Nov 18;800:157-74.
15. Tromp G, Gatalica Z, Skunca M, Berguer R, Siegel T, Kline RA, et al. Elevated expression of matrix metalloproteinase-13 in abdominal aortic aneurysms. Ann Vasc Surg. 2004 Jul;18(4):414-20.
16. Baxter BT, McGee GS, Shively VP, Drummond IA, Dixit SN, Yamauchi M, et al. Elastin content, cross-links, and mRNA in normal and aneurysmal human aorta. J Vasc Surg. 1992 Aug;16(2):192-200.
17. Dobrin PB, Mrkvicka R. Failure of elastin or collagen as possible critical connective tissue alterations underlying aneurysmal dilatation. Cardiovasc Surg. 1994 Aug;2(4):484-8.
18. Sakalihasan N, Heyeres A, Nusgens BV, Limet R, Lapiere CM. Modifications of the extracellular matrix of aneurysmal abdominal aortas as a function of their size. Eur J Vasc Surg. 1993 Nov;7(6):633-7.
19. Sandiford P, Mosquera D, Bramley D. Trends in incidence and mortality from abdominal aortic aneurysm in New Zealand. British Journal of Surgery. [10.1002/bjs.7461]. 2011;98(5):645-51.
20. Sakalihasan N, Limet R, Defawe OD. Abdominal aortic aneurysm. Lancet. 2005 Apr 30-May 6;365(9470):1577-89.
21. Kniemeyer HW, Kessler T, Reber PU, Ris HB, Hakki H, Widmer MK. Treatment of ruptured abdominal aortic aneurysm, a permanent challenge or a waste of resources? Prediction of outcome using a multi-organ-dysfunction score. European Journal of Vascular and Endovascular Surgery. 2000 Feb;19(2):190-6.
22. Haschek E, Lindelthal OT. Ein Beitrag zur praktischen verwerthung der Photographie nach Rontgen. Wiener Klin Wochenschr. 1896;9:63.
23. Fye WB. Coronary arteriography--it took a long time! Circulation. 1984 Nov;70(5):781-7.
24. Sassard R, O'Leary JP. Egas Moniz: pioneer of cerebral angiography. Am Surg. 1998 Nov;64(11):1116-7.
25. Forssmann W. Die Sondierung des Rechten Herzens. Journal of Molecular Medicine. 1929;8(45):2085-7.
26. Gaylis H, Laws JW. Dissection of Aorta as a Complication of Translumbar Aortography. BMJ. 1956 1956-11-17 00:00:00;2(5002):1141-6.
27. Seldinger SI. Catheter Replacement of the Needle in Percutaneous Arteriography: A new technique. Acta Radiologica [Old Series]. [doi: 10.3109/00016925309136722]. 1953 1953/05/01;39(5):368-76.
28. Coltman JW. Fluoroscopic image brightening by electronic means. Radiology. 1948 Sep;51(3):359-67.

29. Krohmer JS. Radiography and fluoroscopy, 1920 to the present. Radiographics. 1989 Nov;9(6):1129-53.
30. Crummy AB, Stieghorst MF, Turski PA, Strother CM, Lieberman RP, Sackett JF, et al. Digital subtraction angiography: current status and use of intra-arterial injection. Radiology. 1982 November 1, 1982;145(2):303-7.
31. Szilagyi DE, Smith RF, DeRusso FJ, Elliott JP, Sherrin FW. Contribution of abdominal aortic aneurysmectomy to prolongation of life. Ann Surg. 1966 Oct;164(4):678-99.
32. Volodos NL, Shekhanin VE, Karpovich IP, Troian VI, Gur'ev Iu A. [A self-fixing synthetic blood vessel endoprosthesis]. Vestn Khir Im I I Grek. 1986 Nov;137(11):123-5.
33. Parodi JC, Palmaz JC, Barone HD. Transfemoral intraluminal graft implantation for abdominal aortic aneurysms. Ann Vasc Surg. 1991 Nov;5(6):491-9.
34. EVAR Trial p. Endovascular aneurysm repair versus open repair in patients with abdominal aortic aneurysm (EVAR trial 1): randomised controlled trial. The Lancet. [doi: 10.1016/S0140-6736(05)66627-5]. 2005;365(9478):2179-86.
35. Greenhalgh RM, Brown LC, Kwong GP, Powell JT, Thompson SG. Comparison of endovascular aneurysm repair with open repair in patients with abdominal aortic aneurysm (EVAR trial 1), 30-day operative mortality results: randomised controlled trial. Lancet. 2004 Sep 4-10;364(9437):843-8.
36. Geijer H, Larzon T, Popek R, Beckman KW. Radiation exposure in stent-grafting of abdominal aortic aneurysms. British Journal of Radiology. 2005 Oct;78(934):906-12.
37. Morcos SK. Prevention of contrast media-induced nephrotoxicity after angiographic procedures. Journal of Vascular and Interventional Radiology. 2005 Jan;16(1):13-23.
38. Ho P, Cheng SW, Wu PM, Ting AC, Poon JT, Cheng CK, et al. Ionizing radiation absorption of vascular surgeons during endovascular procedures. Journal of Vascular Surgery. 2007 Sep;46(3):455-9.
39. Greenberg RK, West K, Pfaff K, Foster J, Skender D, Haulon S, et al. Beyond the aortic bifurcation: branched endovascular grafts for thoracoabdominal and aortoiliac aneurysms. J Vasc Surg. 2006 May;43(5):879-86; discussion 86-7.
40. Glossop ND. Advantages of optical compared with electromagnetic tracking. J Bone Joint Surg Am. 2009 Feb;91 Suppl 1:23-8.
41. Golfinos JG, Fitzpatrick BC, Smith LR, Spetzler RF. Clinical use of a frameless stereotactic arm: results of 325 cases. J Neurosurg. 1995 Aug;83(2):197-205.
42. Yanying G, Lo A, Niemegeers I. A survey of indoor positioning systems for wireless personal networks. Communications Surveys & Tutorials, IEEE. 2009;11(1):13-32.
43. NDI. Polaris Technical Specifications. http://wwwndigitalcom/medical/polarisfamily-techspecsphp.Accessed 2012 March 23.
44. Yaniv Z, Wilson E, Lindisch D, Cleary K. Electromagnetic tracking in the clinical environment. Medical Physics. 2009;36(3):876-92.

45. Haidegger T, Fenyvesi G, Sirokai B, Kelemen M, Nagy M, Takacs B, et al. Towards unified electromagnetic tracking system assessment-static errors. Conf Proc IEEE Eng Med Biol Soc. 2011;2011:1905-8.
46. Much J. Error Classification and Propagation for Electromagnetic Tracking. MSc thesis in Computer Science, Technical University Munich. 2008.
47. Eberhardt R, Morgan RK, Ernst A, Beyer T, Herth FJ. Comparison of suction catheter versus forceps biopsy for sampling of solitary pulmonary nodules guided by electromagnetic navigational bronchoscopy. Respiration. 2010;79(1):54-60.
48. Harms J, Feussner H, Baumgartner M, Schneider A, Donhauser M, Wessels G. Three-dimensional navigated laparoscopic ultrasonography: first experiences with a new minimally invasive diagnostic device. Surg Endosc. 2001 Dec;15(12):1459-62.
49. Hayhurst C, Byrne P, Eldridge PR, Mallucci CL. Application of electromagnetic technology to neuronavigation: a revolution in image-guided neurosurgery. J Neurosurg. 2009 Dec;111(6):1179-84.
50. Hildebrand P, Schlichting S, Martens V, Besirevic A, Kleemann M, Roblick U, et al. Prototype of an intraoperative navigation and documentation system for laparoscopic radiofrequency ablation: first experiences. European Journal of Surgical Oncology. 2008 Apr;34(4):418-21.
51. Nagelhus Hernes TA, Lindseth F, Selbekk T, Wollf A, Solberg OV, Harg E, et al. Computer-assisted 3D ultrasound-guided neurosurgery: technological contributions, including multimodal registration and advanced display, demonstrating future perspectives. Int J Med Robot. 2006 Mar;2(1):45-59.
52. Tigani D, Busacca M, Moio A, Rimondi E, Del Piccolo N, Sabbioni G. Preliminary experience with electromagnetic navigation system in TKA. Knee. 2009 Jan;16(1):33-8.
53. von Jako RA, Carrino JA, Yonemura KS, Noda GA, Zhue W, Blaskiewicz D, et al. Electromagnetic navigation for percutaneous guide-wire insertion: accuracy and efficiency compared to conventional fluoroscopic guidance. Neuroimage. 2009 Aug;47 Suppl 2(2):T127-32.
54. Wood BJ, Locklin JK, Viswanathan A, Kruecker J, Haemmerich D, Cebral J, et al. Technologies for guidance of radiofrequency ablation in the multimodality interventional suite of the future. Journal of Vascular and Interventional Radiology. 2007 Jan;18(1 Pt 1):9-24.
55. Knecht S, Skali H, O'Neill MD, Wright M, Matsuo S, Chaudhry GM, et al. Computed tomography-fluoroscopy overlay evaluation during catheter ablation of left atrial arrhythmia. Europace. 2008 Aug;10(8):931-8.
56. Abi-Jaoudeh N, Glossop N, Dake M, Pritchard WF, Chiesa A, Dreher MR, et al. Electromagnetic navigation for thoracic aortic stent-graft deployment: a pilot study in swine. Journal of Vascular and Interventional Radiology. 2010 Jun;21(6):888-95.
57. Greenberg RK, Lytle B. Endovascular repair of thoracoabdominal aneurysms. Circulation. 2008 Apr 29;117(17):2288-96.
58. Reilly LM, Chuter TA. Endovascular repair of thoracoabdominal aneurysms: design options, device construct, patient selection and complications. Journal of Cardiovascular Surgery. 2009 Aug;50(4):447-60.

59. McCullough PA, Adam A, Becker CR, Davidson C, Lameire N, Stacul F, et al. Risk prediction of contrast-induced nephropathy. American Journal of Cardiology. 2006 Sep 18;98(6A):27K-36K.
60. Cross J, Gurusamy K, Gadhvi V, Simring D, Harris P, Ivancev K, et al. Fenestrated endovascular aneurysm repair. British Journal of Surgery. 2012 Feb;99(2):152-9.
61. Jones C, Badger SA, Boyd CS, Soong CV. The impact of radiation dose exposure during endovascular aneurysm repair on patient safety. Journal of Vascular Surgery. 2010 Aug;52(2):298-302.
62. NDI. Aurora Technical Spesifications. http://wwwndigitalcom/medical/aurora-techspecs-performancephp. Accessed 2012 Jan 6.
63. Walker TG, Kalva SP, Yeddula K, Wicky S, Kundu S, Drescher P, et al. Clinical practice guidelines for endovascular abdominal aortic aneurysm repair: written by the Standards of Practice Committee for the Society of Interventional Radiology and endorsed by the Cardiovascular and Interventional Radiological Society of Europe and the Canadian Interventional Radiology Association. Journal of Vascular and Interventional Radiology. 2010 Nov;21(11):1632-55.
64. Acher C, Wynn M. Outcomes in open repair of the thoracic and thoracoabdominal aorta. Journal of Vascular Surgery. 2010 Oct;52(4 Suppl):3S-9S.
65. Wong DR, Parenti JL, Green SY, Chowdhary V, Liao JM, Zarda S, et al. Open repair of thoracoabdominal aortic aneurysm in the modern surgical era: contemporary outcomes in 509 patients. J Am Coll Surg. 2011 Apr;212(4):569-79; discussion 79-81.
66. Anderson JL, Berce M, Hartley DE. Endoluminal aortic grafting with renal and superior mesenteric artery incorporation by graft fenestration. J Endovasc Ther. 2001 Feb;8(1):3-15.
67. Stanley BM, Semmens JB, Lawrence-Brown MM, Goodman MA, Hartley DE. Fenestration in endovascular grafts for aortic aneurysm repair: new horizons for preserving blood flow in branch vessels. J Endovasc Ther. 2001 Feb;8(1):16-24.
68. Greenberg RK, Sternbergh WC, 3rd, Makaroun M, Ohki T, Chuter T, Bharadwaj P, et al. Intermediate results of a United States multicenter trial of fenestrated endograft repair for juxtarenal abdominal aortic aneurysms. Journal of Vascular Surgery. 2009 Oct;50(4):730-7 e1.
69. Wald R, Waikar SS, Liangos O, Pereira BJ, Chertow GM, Jaber BL. Acute renal failure after endovascular vs open repair of abdominal aortic aneurysm. Journal of Vascular Surgery. 2006 Mar;43(3):460-6; discussion 6.
70. Detrenis S, Meschi M, Bertolini L, Savazzi G. Contrast medium administration in the elderly patient: is advancing age an independent risk factor for contrast nephropathy after angiographic procedures? Journal of Vascular and Interventional Radiology. 2007 Feb;18(2):177-85; quiz 85.
71. Eide KR, Odegard A, Myhre HO, Lydersen S, Hatlinghus S, Haraldseth O. DynaCT during EVAR - A Comparison with Multidetector CT. European Journal of Vascular and Endovascular Surgery. 2008 Nov 14.
72. Mitsui T, Fujii M, Tsuzaka M, Hayashi Y, Asahina Y, Wakabayashi T. Skin shift and its effect on navigation accuracy in image-guided neurosurgery. Radiol Phys Technol. 2011 Jan;4(1):37-42.

73. Fitzpatrick JM, West JB, Maurer CR, Jr. Predicting error in rigid-body point-based registration. IEEE Transactions on Medical Imaging. 1998 Oct;17(5):694-702.
74. Fitzpatrick JM, editor. Fiducial registration error and target registration error are uncorrelated2009: SPIE.
75. Wood BJ, Zhang H, Durrani A, Glossop N, Ranjan S, Lindisch D, et al. Navigation with electromagnetic tracking for interventional radiology procedures: a feasibility study. Journal of Vascular and Interventional Radiology. 2005 Apr;16(4):493-505.
76. Brown LC, Powell JT, Thompson SG, Epstein DM, Sculpher MJ, Greenhalgh RM. The UK EndoVascular Aneurysm Repair (EVAR) trials: randomised trials of EVAR versus standard therapy. Health Technology Assessment. 2012;16(9):1-218.
77. Reilly LM, Rapp JH, Grenon SM, Hiramoto JS, Sobel J, Chuter TA. Efficacy and durability of endovascular thoracoabdominal aortic aneurysm repair using the caudally directed cuff technique. J Vasc Surg. 2012 Jul;56(1):53-64.

12 PAPERS 1-4

Paper I

Is not included due to copyright

Paper II

Is not included due to copyright

Paper III

◆ EXPERIMENTAL INVESTIGATION ◆

Three-Dimensional Endovascular Navigation With Electromagnetic Tracking: Ex Vivo and In Vivo Accuracy

Frode Manstad-Hulaas, MD[1]; Geir Arne Tangen, MSc[2]; Lucian Gheorghe Gruionu, MSc, PhD[3]; Petter Aadahl, MD, PhD[1]; and Toril A. N. Hernes, MSc, PhD[1,2]

[1]Department of Circulation and Medical Imaging, Faculty of Medicine, Norwegian University of Science and Technology, Trondheim, Norway. [2]SINTEF Technology and Society, Department Medical Technology, Trondheim, Norway. [3]Faculty of Engineering and Management of Technological Systems, University of Craiova, Drobeta Turnu Severin, Romania.

Purpose: To evaluate the accuracy of a 3-dimensional (3D) navigation system using electromagnetically tracked tools to explore its potential in patients.
Methods: The 3D navigation accuracy was quantified on a phantom and in a porcine model using the same setup and vascular interventional suite. A box-shaped phantom with 16 markers was scanned in 5 different positions using computed tomography (CT). The 3D navigation system registered each CT volume in the magnetic field. A tracked needle was pointed at the physical markers, and the spatial distances between the tracked needle positions and the markers were calculated. Contrast-enhanced CT images were acquired from 6 swine. The 3D navigation system registered each CT volume in the magnetic field. An electromagnetically tracked guidewire and catheter were visualized in the 3D image and navigated to 4 specified targets. At each target, the spatial distance between the tracked guidewire tip position and actual position, verified by a CT control, was calculated.
Results: The mean accuracy on the phantom was 1.28 $\pm$ 0.53 mm, and 90% of the measured distances were $\leq$1.90 mm. The mean accuracy in swine was 4.18 $\pm$ 1.76 mm, and 90% of the measured distances were $\leq$5.73 mm.
Conclusion: This 3D navigation system demonstrates good ex vivo accuracy and is sufficiently accurate in vivo to explore its potential for improved endovascular navigation.
J Endovasc Ther. 2011;18:000–000

Key words: electromagnetic tracking, navigation, endovascular aneurysm repair, abdominal aortic aneurysm, image-guided surgery, angioplasty, interventional radiography, radiological technology

The surgical repair of thoracoabdominal aortic aneurysms (TAAAs) is encumbered by numerous complications (visceral, spinal cord, and myocardial ischemia; pulmonary edema; and renal failure) and has a mortality risk that ranges from 3% to 17%.[1,2] Endovascular aneurysm repair (EVAR) has several advantages over open repair, and some centers have gained experience with the endovascular repair of TAAAs[3,4] to reduce

This study received financial support and equipment from the Research Council of Norway, the FRIMED Program, the National Center of Competence for 3D Ultrasound in Surgery, SINTEF Department of Medical Technology, the Norwegian University of Science and Technology, and St Olav's Hospital.

The authors have no commercial, proprietary, or financial interest in any products or companies described in this article.

Address for correspondence and reprints: Frode Manstad-Hulaas, Department of Circulation and Medical Imaging, Faculty of Medicine, Norwegian University of Science and Technology, Post Box 8905 MTFS, 7491 Trondheim, Norway. E-mail: *frode.manstad.hulaas@ntnu.no*

the morbidity and mortality associated with surgery. The anatomical conditions complicate the endovascular repair of TAAAs, which results in a prolonged operation time and an increased exposure to radiation and contrast medium.[5,6] Exposure of EVAR patients to substantial radiation[7] stresses the importance of limiting the radiation time in more complex procedures.

To decrease the use of radiation and contrast medium, yet allow safe insertion and alignment of the stent-graft and targeting of the visceral arteries, a navigation system based on 3-dimensional (3D) images and electromagnetically (EM)–tracked guidewires and catheters can be applied.[8,9] The use of 3D images and EM-tracked devices has been previously tested and applied in a wide range of surgical specialties to offer more anatomical information and make navigation easier, safer, and more accurate.[10–18] Furthermore, some ex vivo studies, animal experiments, and a case report[8,9,19–21] have demonstrated the use of 3D images and electromagnetic tracking in endovascular interventions.

A possible reason for the somewhat late discovery of 3D navigation in endovascular procedures is that fluoroscopic and angiographic guidance, despite the required radiation and contrast, is a well-known and established technique that demonstrates a high success rate in most current procedures. In addition, further refinement and a full and user-friendly integration of 3D navigation technology, intraoperative imaging, and interventional tools, such as EM-tracked catheters and guidewires, is necessary.

If a navigation system based on 3D images and EM-tracked tools are to be a helpful supplement to conventional fluoroscopy and angiography in complicated endovascular procedures, such as TAAA repair, the accuracy of the system must be tested. The aim of the present study was to quantify the accuracy of a prototype 3D navigation system in a clinical environment prior to exploring its potential for improved guidance in endovascular procedures. The accuracy was first quantified ex vivo on a phantom and then in vivo on a porcine model, using the same setup and vascular interventional suite.

METHODS

Electromagnetic Tracking System

The tracking system (Aurora; Northern Digital Inc., Waterloo, ON, Canada) used in the present setup comprised an electromagnetic generator, control box, and electromagnetically-tracked position sensors (Fig. 1A–D). The electromagnetic generator was placed underneath the operating table; it generated a magnetic field that measured $\sim 0.5 \times 0.5 \times 0.5$ m^3. The position sensors had 5 or 6 degrees of freedom (DOF) and measured 0.5×8 mm and 1.8×9 mm, respectively. A 6-DOF sensor has a better position accuracy in comparison to a 5-DOF sensor (0.6 mm versus 0.9 mm; http://www.ndigital.com/medical/aurora-techspecs-performance.*php*) and also provides rotation, but the larger diameter of a 6-DOF sensor makes it unsuitable for integration in some instruments. When a sensor was placed within the magnetic field, a current was induced and used to calculate the position of the sensor relative to the electromagnetic generator. The sensors were embedded into the necessary tools.

Image Acquisition and Registration in the Tracking Space

Computed tomography (CT) data with and without contrast injection were acquired using a roof-mounted cone-beam CT (Siemens AXIOM Artis dTA; Siemens AG Healthcare Section, Forchheim, Germany), which was installed at the vascular interventional suite (Fig. 2), and a Leonardo Workstation (Siemens AG Healthcare Section) was used to reconstruct the data into CT volumes that measured $\sim 21.5 \times 21.5 \times 18.5$ cm with a voxel resolution of 0.627 mm^3. A $10 \times 4 \times 0.5$-cm reference plate was made of polyetheretherketone plastic, and 2 5-DOF sensors and 7 radiopaque spheres were embedded in this plate in a specified configuration (Fig. 3A). This reference plate was placed on the operating table underneath the phantom or swine in a position that ensured the reference plate would be included in all the CT volumes, and it was later used to register the CT image in the magnetic field. The CT volume was transferred to the in-house prototype navigation system (CustusX; SINTEF Technology and Society, Medical Tech-

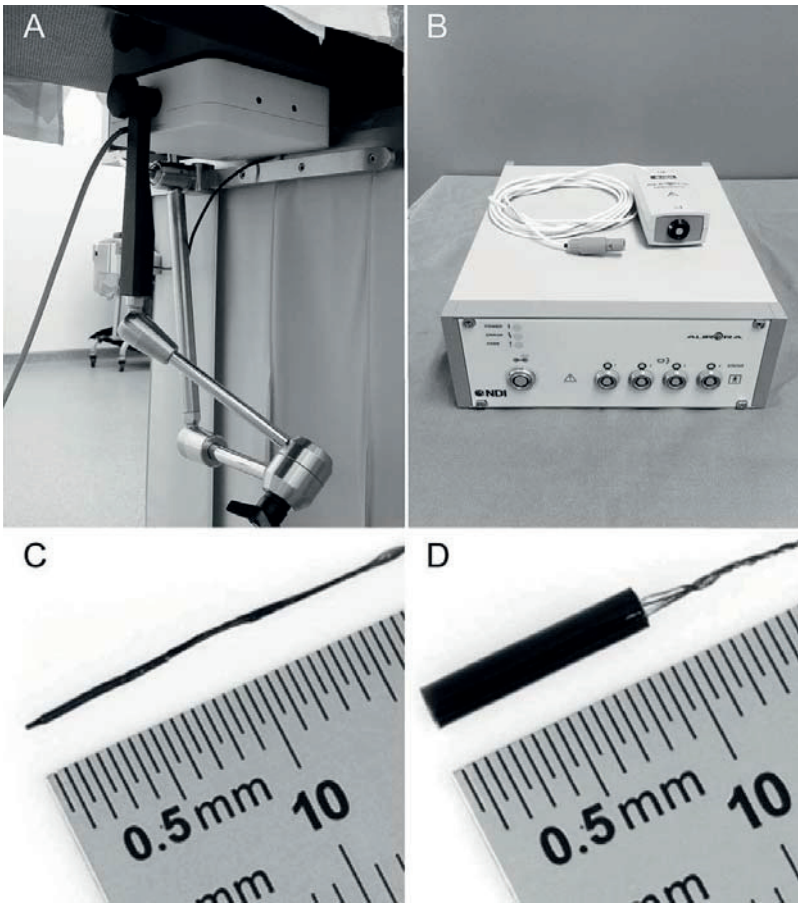

Figure 1 ◆ (**A**) The electromagnetic generator induces an electromagnetic field of approximately 0.5×0.5×0.5 m^3; it was placed underneath the operating table for the vascular interventional setup. (**B**) Up to 4 position sensors and the electromagnetic generator were connected to the control box, which calculated the position of each sensor within the electromagnetic field. (**C, D**) 5-DOF and 6-DOF sensors. Depending on the electric current induced in a sensor within the electromagnetic field, the 3D position can be determined. A 6-DOF sensor also provides all 3 angles of rotation.

nology, Trondheim, Norway). Volume rendering was performed before the CT volume was visualized as a 3D image on the navigation screen. To provide both the position and the orientation of the reference plate, the 2 5-DOF sensors were configured as a single 6-DOF sensor. The 7 radiopaque spheres in the reference plate could then be visualized as green dots on the navigation screen, which indicated their positions in the magnetic field. A manual registration was performed as the CT image was translated within the magnetic field until the radiopaque spheres in the CT image overlaid the corresponding spheres (green dots) in the magnetic field (Fig. 3B). This process resulted in a rigid-body registration between the magnetic field and the CT image space.

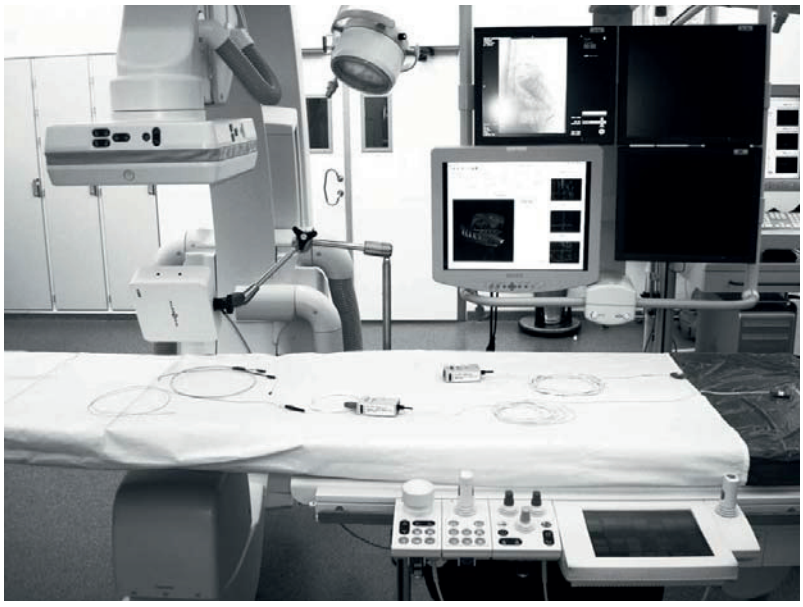

Figure 2 ◆ Setup in the interventional suite. The cone-beam CT was used to acquire the CT volumes. The lower left screen was used for the 3D navigation, and the electromagnetically tracked guidewire and catheter are apparent on the operating table. The electromagnetic generator was mounted underneath the operating table during the interventions, but it was placed above the table in this figure to better illustrate the setup.

Ex Vivo Navigation Accuracy

For the accuracy measurements, a rectangular box-shaped phantom (SINTEF Technology and Society, Medical Technology) that measured 17.5×15×23.5 cm was used. In addition to 8 pin markers inside the phantom, 8 external radiopaque markers were attached to the box-shaped phantom (large image in Fig. 4). The reference plate was placed on the operating table under the phantom. With the electromagnetic generator placed underneath the OR table just below the phantom, the ''navigation volume'' was well within the boundaries of the magnetic field. The navigation volume was the volume of interest, e.g., the area around the renal arteries. Five cone-beam CT scans were performed with the phantom in 5 different positions (the phantom was placed at different oblique angles and tilted). Because the aim of the study was to quantify the mean accuracy within the navigation volume only, different phantom positions were used to spread the phantom markers within the navigation volume. After each cone-beam CT scan, the 3D image was displayed on the navigation screen and manually registered in the magnetic field using the reference plate. A needle with a 6-DOF position sensor embedded in the tip (small image in Fig. 4) was calibrated using the ''pivot tool'' (NDI Toolbox version 3.005.009, Northern Digital Inc., Waterloo, ON, Canada) to determine the x, y, and z offset from the sensor to the needle tip. This calibration was used by the navigation system to report the position data for the needle tool, which was then pointed at the physical phantom markers, and the needle tip positions in the CT image space were marked and saved. The positions of the same phantom markers were then marked in the CT image space using OsiriX (OsiriX version 3.2.1), which is an open-source software DICOM viewer. Finally the spatial distances between the saved needle tip positions and the actual

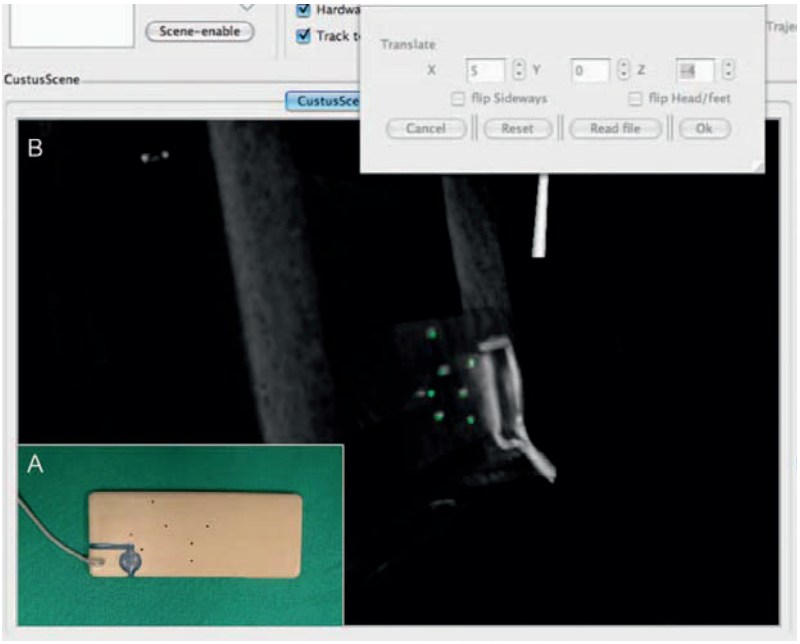

Figure 3 ◆ (**A**) The 7 metallic spheres in the reference plate, together with two 5-DOF electromagnetic sensors, enabled the registration of a CT image space in the magnetic field. (**B**) The 7 metal spheres that were cast in the reference plate were displayed as green dots in the magnetic field. A CT image space was manually registered in the magnetic field by moving the CT image until the metal spheres in the image covered the corresponding green spheres in the magnetic field.

marker positions in the CT volume were calculated (Fig. 5).

In Vivo Navigation Accuracy

Domestic swine that weighed ~60 kg were used in this study (n=6). All of the animals were treated according to the *Guide for the Care and Use of Laboratory Animals*, and the Institutional Animal Care and Use Committee approved the study protocol. The swine were restrained in a supine position with the reference plate attached to their backs at approximately the level of the renal arteries. The interventional suite setup was the same as that previously described for the phantom study. A 5-DOF sensor was integrated into the tip of a custom-made guidewire[22] and a balloon catheter that was modified in our laboratory. The catheter had 2 lumens, one of which was occupied by the position sensor integrated in the catheter tip. A left common carotid arterial access was established using a 6-F introducer system (Radiofocus Introducer II; Terumo Corporation, Tokyo, Japan). Three-dimensional CT angiographies (3D CTA) were acquired with a carotid injection of 100 Ml of contrast medium (Visipaque 270 mg I/mL; GE Healthcare, Chalfont St Giles, UK). The CT data were transferred to the navigation system, and the aorta and branching vessels were visualized by modifying the threshold setting. Then the CTAs were displayed as a 3D image on the navigation screen. A registration between the magnetic field and the CT image space was established using the reference plate and the same manual method as that described for the phantom. The catheter and guidewire were inserted through the carotid access and their tips

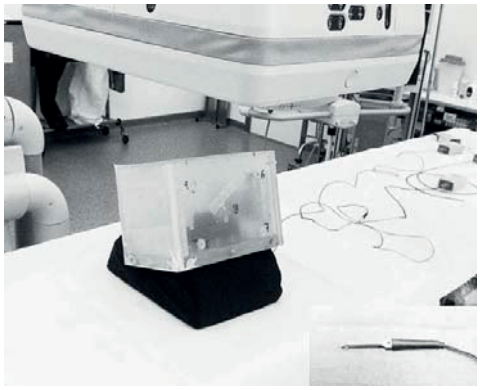

Figure 4 ◆ Rectangular box-shaped phantom and electromagnetically tracked needle. A total of 16 markers that were located both outside and inside the phantom were used. A reference plate was placed underneath the phantom. The CT acquisitions were obtained with the phantom in 5 different positions to distribute the markers throughout the navigation volume. The needle, which was equipped with a 6-DOF sensor, was used to point at the physical phantom markers. While pointing at a physical marker, the tracked needle tip position in the 3D navigation image was marked and saved.

visualized in the 3D image on the navigation screen. With real-time tracking of the sensors, the guidewire and catheter were navigated through the vascular tree (Fig. 6). The guidewire was navigated to and placed at 4 specified targets as shown in the 3D navigation images: orifice of the celiac trunk, orifice of the superior mesenteric artery, and orifices of both renal arteries.

If an arterial branch was missing in the 3D navigation image, another orifice was selected, e.g., if the celiac trunk was missing, the inferior mesenteric artery or a more peripheral branch of the arteries covered in the CT image was used. When the guidewire was placed at a target, the EM-tracked position observed in the 3D navigation image was marked and saved. To investigate the actual position of the guidewire tip in the CT image space, a non-contrasted CT control followed, and the guidewire tip position was marked using OsiriX in the same manner as that previously described for the phantom markers. The CT control was then manually registered in the 3D navigation image (initial CTA) using the reference plate. Both the EM-tracked and actual position of the guidewire tip in the CT image space were visualized, and the spatial distance was calculated (Fig. 7). The workflow is illustrated in Figure 8.

Statistical Analysis

The accuracy of the 3D navigation system is presented as the mean distance ± SD, median, range, and the distance covering 90% of all measured distances. All statistical analyses were computed using SPSS (version 18.0; SPSS Inc., Chicago, IL, USA).

RESULTS

Navigation Accuracy – Ex Vivo

In total, 57 phantom markers were registered. The spatial distances between the marker positions in the magnetic field (needle tip positions) and the marker positions in the CT image space were calculated. The mean distance was 1.28 ± 0.53 mm (median 1.23 mm). The distances ranged from 0.57 to 2.98 mm, and 90% of the measured distances were ≤1.90 mm (Fig. 9A). Due to the different phantom positions, 23 markers were not covered in all of the CT volumes and were excluded from the analysis.

Navigation Accuracy – In Vivo

In total, 24 guidewire tip positions were registered. The spatial distances between the guidewire tip positions in the 3D navigation image and the CT controls were calculated. The mean distance was 4.18 ± 1.76 mm (median 3.99 mm). The distances ranged from 1.57 to 8.88 mm, and 90% of all of the measured distances were ≤5.73 mm (Fig. 9B).

DISCUSSION

When a new technology is introduced, accuracy is an important factor in its successful implementation in medical interventions. The accuracy referred to in the present study reflects the degree of conformity found

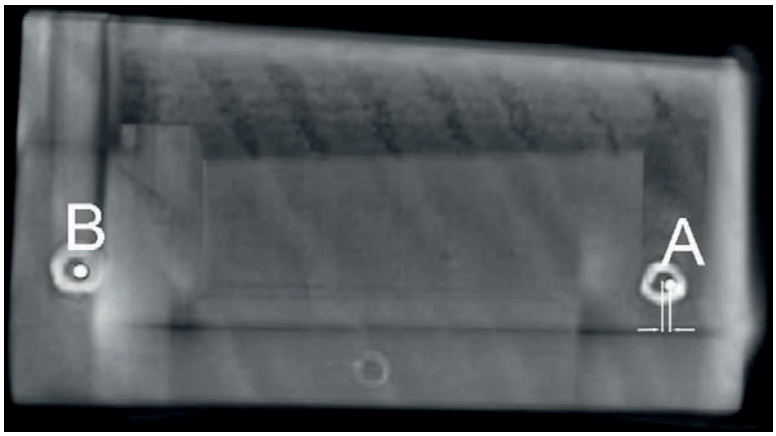

Figure 5 ◆ Measurements of the navigation accuracy on the phantom. Points A and B are 2 phantom markers. As the needle tool was pointed at the center of phantom marker A, the tracked needle tip position in the CT image was marked and saved (gray dot inside marker A). The two straight gray lines illustrate the spatial distance between the actual marker position and the needle tip position. The spatial distances between the tracked and actual marker positions were calculated.

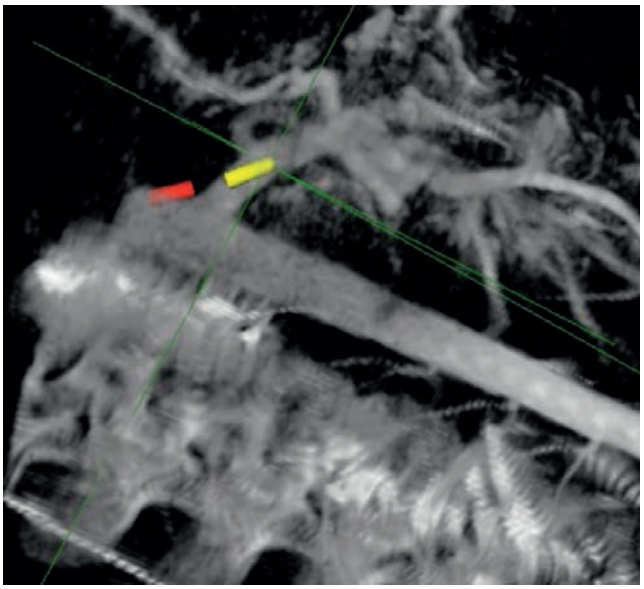

Figure 6 ◆ The tip of the guidewire (yellow) and catheter (red) were visualized in the 3D navigation image during navigation into the superior mesenteric artery of a swine. The navigation was performed in real time, and the 3D image could be rotated and zoomed in or out. The degree of image opacity during the navigation could also be modulated.

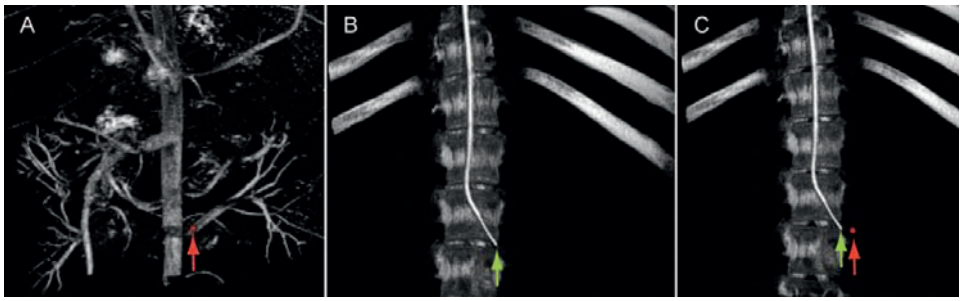

Figure 7 ◆ Measurements of the navigation accuracy in swine. (**A**) The left figure shows the 3D navigation image, in which the red arrow indicates the marked and saved guidewire tip position. (**B**) The figure shows the CT control, in which the green arrow indicates the actual guidewire tip position in the CT image space. (**C**) After co-registration of the 3D navigation image and the CT control, the electromagnetically tracked and actual guidewire tip positions were visualized (red and green arrows), and the spatial distance between them was calculated.

between EM-tracked positions in the navigation system and their corresponding positions in the CT image space. In navigation systems this type of accuracy is often referred to as target registration error (TRE). In this study, the ex vivo accuracy was comparable to those determined by others,[23,24] whereas the in vivo accuracy was almost identical to the results reported by Abi-Jaoudeh et al.[9]

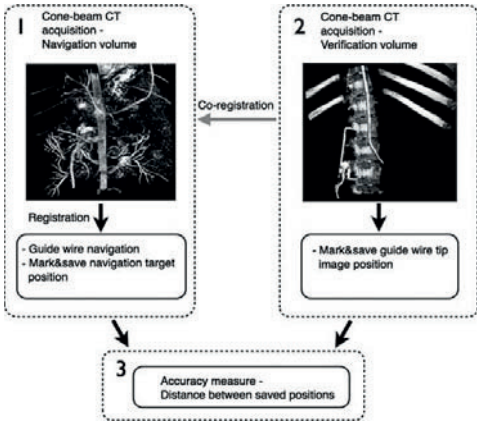

Figure 8 ◆ In vivo study workflow. (**1**) A CT angiogram was acquired and used as the 3D navigation image, which was registered in the magnetic field before a guidewire was navigated to a predetermined target. When the target was reached, the tracked guidewire tip position in the CT image was marked and saved. (**2**) A CT control was performed, and the actual guidewire tip position was marked and saved. (**3**) Finally, the CT control and navigation volume were co-registered to measure the spatial distance between the saved positions, i.e., the distance between the tracked and the actual positions of the guidewire tip.

In neurosurgery, an accuracy of 5 mm for electromagnetic navigation systems is deemed acceptable.[25] The estimated in vivo accuracy of ~4 mm determined in this study should allow further exploration of the potential of 3D navigation systems in clinical endovascular procedures. However, the results were also influenced by different sources of error that could be further reduced. When using a reference plate with beads in a known configuration that are clearly visible in a CT image, the fiducial localization error (FLE) is expected to be minimized. However, the manual registration of the radiopaque spheres in a CT image to the corresponding spheres in the magnetic field still contained a fiducial registration error (FRE). The FRE in our study could be reduced by the introduction of an automated registration process. In regards to FRE and FLE, it is important to be aware of that the expected TRE, which is the displacement from the true position of a registered point not used as a fiducial, is related to FLE but uncorrelated to FRE.[26] Although FRE cannot be used as an estimate for TRE, a FRE value higher than usual indicates a larger than usual probability that the navigation system is malfunctioning.

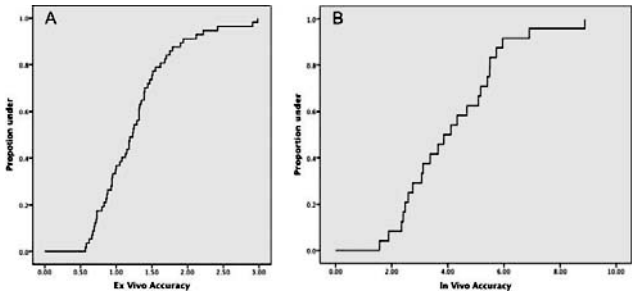

Figure 9 ◆ The distribution of the ex vivo (**A**) and in vivo (**B**) accuracy measurements followed a relatively straight curve, but both were characterized by some outliers. Ninety percent of the measured distances were ≤1.90 mm for the ex vivo study and ≤5.73 mm for the in vivo study.

Furthermore, to assess the actual guidewire tip positions in the CT image space, the CT controls were manually registered in the navigation volumes (rigid volume-volume registration). This registration also contained an error that affected the results. The tracked needle tool was calibrated using calibration software from Northern Digital Inc. (NDI), but the guidewire was calibrated manually in our laboratory. Together with the basic sensor position error (accuracy 0.9 mm according to NDI, estimated under optimal conditions), the calibration error influences the overall accuracy measured. Another factor that influences the electromagnetic tracking accuracy is the presence of ferromagnetic metals.[27] This phenomenon is well known, and it was minimized in the present study, as the C-arm was excluded from the vicinity of the electromagnetic field during navigation.

Because the EM-tracked positions were recorded before the CT controls were conducted, we cannot exclude the possibility that the guidewire could have moved from its original position due to blood flow and pulsation in the arteries. This event may have affected the present results. Both the phantom and the swine were placed on a mattress that minimized patient movement, but minor alterations can always occur during a procedure. However, when the guidewire and catheter were navigated to the different arterial orifices and to more peripheral vessel branches, these targets were easily reached, although the measured in vivo error was relatively large. We observed a good compliance between the sensors (guidewire and catheter tips) and the 3D navigation image, which indicated that the sensors moved almost constantly within the arterial walls as observed in the CT image, even within the more peripheral arteries (diameter of ~3–7 mm). This finding is inconsistent with the largest error obtained (8.88 mm) and might indicate that the calculated error was overestimated. In addition, the accuracy was measured at specific positions and not over the entire navigation volume.

With respect to clinical usefulness and safety, transparency and the interpretation of information are important factors. We believe that a mean accuracy of ~4 mm is sufficient to provide valuable information in most interventions.

For practical reasons, a common carotid arterial access was selected when navigation accuracy was evaluated in swine. This approach certainly does not contradict a brachial or femoral access in humans. Although 3D images and new tools for endovascular navigation may become helpful in endovascular interventions, it is unlikely that 3D navigation systems will replace fluoroscopic imaging, at least not in the near future. However, 3D images and navigation may provide valuable additional information and lower the threshold for difficult procedures such as TAAA repair. In our experience, 3D navigation technology has matured, and with the improved accuracy of the navigation system, clinical endovascular feasibility studies should be initiated.

Conclusion

Navigation and 3D images provide valuable guidance assistance during endovascular procedures. Given the satisfactory navigation accuracy, the use of navigation systems based on 3D images and EM-tracked tools could become applicable in complicated endovascular procedures such as TAAA repair. They may also prove to be a valuable supplement in the guidance of routine EVAR.

Acknowledgments: We thank the Research Council of Norway, the FRIMED Program, the National Center of Competence for 3D Ultrasound in Surgery, SINTEF Department of Medical Technology, the Norwegian University of Science and Technology, and St Olav's Hospital for their support of this work.

REFERENCES

1. Reilly LM, Chuter TA. Endovascular repair of thoracoabdominal aneurysms: design options, device construct, patient selection and complications. *J Cardiovasc Surg*. 2009;50:447–460.
2. Greenberg RK, Lytle B. Endovascular repair of thoracoabdominal aneurysms. *Circulation*. 2008; 117:2288–3396.
3. Ferreira M, Lanziotti L, Monteiro M. Branched devices for thoracoabdominal aneurysm repair: Early experience. *J Vasc Surg*. 2008;48: 30S–36S.
4. Greenberg RK, Sternbergh WC, Makaroun M, et al. Intermediate results of a United States multicenter trial of fenestrated endograft repair for juxtarenal abdominal aortic aneurysms. *J Vasc Surg*. 2009;50:730–737.
5. Gilling-Smith GL, McWilliams RG, Scurr JR, et al. Wholly endovascular repair of thoracoabdominal aneurysm. *Br J Surg*. 2008;95: 703–708.
6. Chuter TA, Rapp JH, Hiramoto JS, et al. Endovascular treatment of thoracoabdominal aortic aneurysms. *J Vasc Surg*. 2008;47:6–16.
7. Geijer H, Larzon T, Popek R, et al. Radiation exposure in stent-grafting of abdominal aortic aneurysms. *Br J Radiol*. 2005;78:906–912.
8. Manstad-Hulaas F, Ommedal S, Tangen GA, et al. Side-branched AAA stent graft insertion using navigation technology: a phantom study. *Eur Surg Res*. 2007;39:364–371.
9. Abi-Jaoudeh N, Glossop N, Dake M, et al. Electromagnetic navigation for thoracic aortic stent-graft deployment: a pilot study in swine. *J Vasc Interv Radiol*. 2010;21:888–895.
10. Eberhardt R, Morgan RK, Ernst A, et al. Comparison of suction catheter versus forceps biopsy for sampling of solitary pulmonary nodules guided by electromagnetic navigational bronchoscopy. *Respiration*. 2010;79:54–60.
11. Harms J, Feussner H, Baumgartner M, et al. Three-dimensional navigated laparoscopic ultrasonography: first experiences with a new minimally invasive diagnostic device. *Surg Endosc*. 2001;15:1459–1462.
12. Hayhurst C, Byrne P, Eldridge PR, et al. Application of electromagnetic technology to neuronavigation: a revolution in image-guided neurosurgery. *J Neurosurg*. 2009;111:1179–1184.
13. Hildebrand P, Schlichting S, Martens V, et al. Prototype of an intraoperative navigation and documentation system for laparoscopic radiofrequency ablation: first experiences. *Eur J Surg Oncol*. 2008;34:418–421.
14. Nagelhus Hernes TA, Lindseth F, Selbekk T, et al. Computer-assisted 3D ultrasound-guided neurosurgery: technological contributions, including multimodal registration and advanced display, demonstrating future perspectives. *Int J Med Robot*. 2006;2:45–59.
15. Tigani D, Busacca M, Moio A, et al. Preliminary experience with electromagnetic navigation system in TKA. *Knee*. 2009;16:33–38.
16. von Jako RA, Carrino JA, Yonemura KS, et al. Electromagnetic navigation for percutaneous guide-wire insertion: accuracy and efficiency compared to conventional fluoroscopic guidance. *Neuroimage*. 2009;47:T127–T132.
17. Wood BJ, Locklin JK, Viswanathan A, et al. Technologies for guidance of radiofrequency ablation in the multimodality interventional suite of the future. *J Vasc Interv Radiol*. 2007; 18:9–24.
18. Knecht S, Skali H, O'Neill MD, et al. Computed tomography-fluoroscopy overlay evaluation during catheter ablation of left atrial arrhythmia. *Europace*. 2008;10:931–938.
19. Manstad-Hulaas F, Tangen GA, Ødegård A, et al. Interventional Radiology Suite of the Future. *Proc IJCARS*. 2008;3:64–67.
20. Wood BJ, Zhang H, Durrani A, et al. Navigation with electromagnetic tracking for interventional radiology procedures: a feasibility study. *J Vasc Interv Radiol*. 2005;16:493–505.
21. Penzkofer T, Bruners P, Isfort P, et al. Vascular electromagnetic tracking: experiences in phantom and animal cadaveric models. *Proc IFMBE*. 2009;25:232–234.
22. Gruionu L, Manstad-Hulaas F, Wilson E, et al. Surgical Robotics, instrumentation and navigation. *Proc IJCARS*. 2008;3:119–125.

23. Hoheisel M, Skalej M, Beuing O, et al. Kyphoplasty interventions using a navigation system and C-arm CT data: first clinical results. *Proc SPIE*. 2009;7258:72580E1–72580E8.
24. Nagel M, Hoheisel M, Petzold R, et al. Needle and catheter navigation using electromagnetic tracking for computer-assisted C-arm CT interventions. *Proc SPIE*. 2007;6509:65090J1–65090J9.
25. Zaaroor M, Bejerano Y, Wenfeld Z, et al. Novel magnetic technology for intraoperative intracranial frameless navigation: in vivo and in vitro results. *Neurosurgery*. 2001;48:1100–1108.
26. Fitzpatrick JM. Fiducial registration error and target registration error are uncorrelated. *Proc SPIE*. 2009;7261:726102–1–726102-12.
27. Schicho K, Figl M, Donat M, et al. Stability of miniature electromagnetic tracking systems. *Phys Med Biol*. 2005;50:2089–2098.

Paper IV

◆ CLINICAL INVESTIGATION ◆

Three-Dimensional Electromagnetic Navigation vs. Fluoroscopy for Endovascular Aneurysm Repair: A Prospective Feasibility Study in Patients

Frode Manstad-Hulaas, MD[1,3]; Geir Arne Tangen, MSc[2]; Torbjørn Dahl, MD[1,4]; Toril A. N. Hernes, MSc, PhD[1,2]; and Petter Aadahl, MD, PhD[1,5]

[1]Department of Circulation and Medical Imaging, Faculty of Medicine, Norwegian University of Science and Technology, Trondheim, Norway. [2]SINTEF Technology and Society, Department of Medical Technology, Trondheim, Norway. Departments of [3]Radiology, [4]Vascular Surgery, and [5]Cardiothoracic Anesthesia and Intensive Care, St Olavs Hospital, Trondheim, Norway.

Purpose: To evaluate the in vivo feasibility of a 3-dimensional (3D) electromagnetic (EM) navigation system with electromagnetically-tracked catheters in endovascular aneurysm repair (EVAR).

Methods: The pilot study included 17 patients undergoing EVAR with a bifurcated stent-graft. Ten patients were assigned to the control group, in which a standard EVAR procedure was used. The remaining 7 patients (intervention group) underwent an EVAR procedure during which a cone-beam computed tomography image was acquired after implantation of the main stent-graft. The 3D image was presented on the navigation screen. From the contralateral side, the tip of an electromagnetically-tracked catheter was visualized in the 3D image and positioned in front of the contralateral cuff in the main stent-graft. A guidewire was inserted through the catheter and blindly placed into the stent-graft. The placement of the guidewire was verified by fluoroscopy before the catheter was pushed over the guidewire. If the guidewire was incorrectly placed outside the stent-graft, the procedure was repeated. Successful placement of the guidewire had to be achieved within a 15-minute time limit.

Results: Within 15 minutes, the guidewire was placed correctly inside the stent-graft in 6 of 7 patients in the intervention group and in 8 of 10 patients in the control group. In the intervention group, fewer attempts were needed to insert the guidewire correctly.

Conclusion: A 3D EM navigation system, used in conjunction with fluoroscopy and angiography, has the potential to provide more spatial information and reduce the use of radiation and contrast during endovascular interventions. This pilot study showed that 3D EM navigation is feasible in patients undergoing EVAR. However, a larger study must be performed to determine if 3D EM navigation is better than the existing practice for these patients.

J Endovasc Ther. 2012;19:000–000

Key words: electromagnetic tracking, navigation, endovascular aneurysm repair, abdominal aortic aneurysm, image-guided surgery, angioplasty, interventional radiography, radiologic technology

The study was funded in part by the Research Council of Norway through the FIFOS Program Project 152831/530, the FRIMED Program Project 196726/V50, the National Center of Competence for 3D Ultrasound in Surgery, SINTEF Department of Medical Technology, the Norwegian University of Science and Technology, and the Operating Room of the Future at St Olavs Hospital.

The authors have no commercial, proprietary, or financial interest in any products or companies described in this article.

Corresponding author: Frode Manstad-Hulaas, MD, Department of Circulation and Medical Imaging, Faculty of Medicine, Norwegian University of Science and Technology, Post Box 8905 MTFS7491 Trondheim, Norway. E-mail: *frode.manstad.hulaas@ntnu.no*

During endovascular aneurysm repair (EVAR), conventional fluoroscopic and angiographic images are used to visualize vascular anatomy and guide the maneuvers of different devices (e.g., stent-graft, catheters, and guidewires). Optimal visualization is important in order to achieve correct alignment of the stent-graft and to conduct the intervention as smoothly and safely as possible. In the endovascular treatment of most abdominal and thoracic aortic aneurysms, fluoroscopy has been deemed sufficient for intraoperative visualization. In more complicated aneurysms, i.e., thoracoabdominal aortic aneurysms (TAAAs), the endovascular approach is significantly more challenging. Access from both femoral and brachial arteries is frequently needed, several visceral arteries may have to be catheterized, and the traditional visualization technique is sometimes insufficient. In addition, customized stent-grafts with scallops, fenestrations, and/or directional cuffs are usually a necessity.[1,2] The radiation dose and contrast load also increase considerably, in addition to that incurred in the follow-up computed tomography (CT) scans.[3,4] Radiation and contrast may constitute a health hazard, especially in younger patients and those with comorbidities, such as diabetes mellitus and chronic renal disease.[5] Because of these factors, many complicated aortic aneurysms are treated with standard surgical techniques.

A navigation system with 3-dimensional (3D) electromagnetic (EM) tracking of catheters and guidewires may improve both the overview and guidance capabilities during difficult procedures and may also reduce radiation and contrast dose for patients undergoing EVAR. Our group has previously shown the in vitro feasibility of inserting a side-branched stent-graft using 3D EM navigation in combination with fluoroscopy.[6] Further, in an experimental study evaluating the accuracy of a 3D EM navigation system with electromagnetically-tracked catheters and guidewires, we achieved a navigation accuracy of ~4 mm.[7] Another in vivo study in a swine model has shown the successful implantation of thoracic stent-grafts using only electromagnetic navigation.[8] However, to our knowledge, no studies have so far demonstrated the use of navigation technology with electromagnetically-tracked catheters for guidance during EVAR procedures.

The aim of this open, randomized, pilot study was to evaluate the in vivo feasibility of a navigation system with electromagnetically-tracked catheters as an additional visualization tool during EVAR.

METHODS

Study Rationale

When a bifurcated stent-graft is implanted, the main stent-graft is first put into place (usually from the right femoral artery/ipsilateral side). A catheter and a guidewire are then inserted (usually from the left femoral artery/contralateral side) into the cuff in the main stent-graft to enable implantation of the contralateral limb. Catheterization of the main stent-graft from the contralateral side was deemed suitable to test the feasibility of using 3D EM navigation in EVAR.

Navigation System

The 3D EM navigation system consisted of a prototype navigation software program (CustusX; SINTEF, Department of Medical Technology, Trondheim, Norway) installed on a Macintosh computer; an electromagnetic tracking system (Aurora; Northern Digital Inc., Waterloo, ON, Canada); and catheters embedded with sensors that could be electromagnetically tracked.

The EM tracking system (Fig. 1) was composed of a control unit that interfaced with the navigation software, position sensor coils, and an EM field generator underneath the operating table that created an EM field covering ~0.5×0.5×0.5 m. All position sensor coils (0.8×11 mm) in the present study had 5 degrees of freedom (5-DOF). The catheter tip was removed, and a 5-DOF position sensor was embedded in the tip, which was then sealed with biocompatible epoxy glue (206-CTH; Dymax Corporation, Torrington, CT, USA). The tracking system calculated the position and orientation of the catheter based

Figure 1 ◆ The electromagnetic (EM) field generator, control box, and position sensors. The EM field generator mounted underneath the operating table induced an EM field measuring ~0.5×0.5×0.5 m. The control box processed the data from the EM field generator and sensors and made it available to the navigation system. The position sensors measured 0.8×11 mm and were embedded in the catheter tips. When a sensor was positioned within the EM field, a weak electrical current was induced, which enabled the tracking software to deduce the catheter's position along the x, y, and z axes.

on the electrical current induced in the position sensor coils placed within the EM field.

Commercially available 7-F catheters (Equalizer Balloon Catheter; Boston Scientific, Natick, MA, USA) with 2 lumens were used to manufacture the tracked catheters in our laboratory (Fig. 2). All of the catheters and the 3D EM navigation system were electrically tested according to the International Electrotechnical Commission 60601 standards, using the most stringent classification (cardiac floating/CF-classification, for applications in which the specific device may come in direct conductive contact with the heart). The position reading from the sensor was calibrated to provide the position of the catheter tip. All catheters were sterilized with low-temperature hydrogen peroxide gas plasma.

Patient Groups

Under a protocol approved by the Regional Committee for Medical Research Ethics, 17 patients undergoing EVAR of an abdominal aortic aneurysm were randomized to either the intervention group (n=7) or the control group (n=10). All patients were ≥60 years without known renal insufficiency, unstable coronary syndrome, or heart failure (New

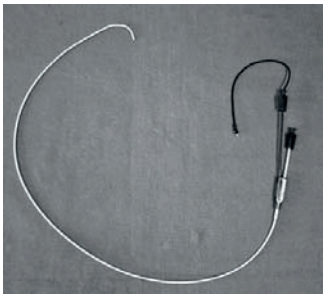

Figure 2 ◆ The 7-F, double lumen, electromagnetically-tracked balloon catheters were 100 cm long. The tip was removed, and a sensor was integrated into the tip before it was resealed with biocompatible epoxy glue. After heating in hot water, the catheter tips were bent at different angles to make them suitable for individual patients.

York Heart Association class 3–4). In the control group, the EVAR procedure was conducted without navigational support.

3D Images and Image Registration

In the intervention group, after implantation of the main stent-graft, an intraoperative CT volume was acquired using a ceiling-mounted C-arm-based cone beam CT (AXIOM Artis dTA; Siemens AG Healthcare Section, Forchheim, Germany) in the angiography suite (Fig. 3). All of the CT volumes included imaging of both the patient as well as the reference plate attached to the patient's back (lumbar region). The reference plate contained 7 radiopaque metal spheres in a known configuration and two 5-DOF sensors (Fig. 4A). The intraoperative CT volumes were then transferred to the navigation system. The threshold settings were manipulated to better display the stent-graft before the CT volumes were presented as a 3D image (256×256 pixels and 441 slices; spatial resolution 0.842×0.842×0.842 mm) on the navigation screen. The two 5-DOF sensors in the reference plate were configured as one 6-DOF sensor that provided position, orientation, and rotation parameters for the reference plate. Because the configuration of the 7 spheres was known, the position of the spheres could be visualized as 7 green dots on the navigation screen, indicating the position and orientation of the reference plate in the EM field. Since the spheres also were visible within the CT images, the 3D image was manually registered by moving it within the EM field until the radiopaque spheres in the 3D image overlaid the corresponding green dots in the EM field as closely as possible (Fig. 4B).

3D EM Navigation

From the contralateral side, the tracked catheter was pushed over a guidewire that had been placed in the descending aorta before deployment of the main stent-graft. An introducer that ended just above the aortic bifurcation was also used to avoid vessel injury from the tracked catheter. As the catheter entered the aneurysm sac, the guidewire was pulled back. The ceiling-mounted C-arm was placed out of the vicinity of the EM field to minimize ferromagnetic interference during navigation. By sliding the operating table, the patient could be moved between the EM field and the C-arm to enable fluoroscopy when required.

Figure 3 ◆ Cone-beam CT. The angiography suite was equipped with a ceiling-mounted Siemens AXIOM Artis dTA imaging system. Images were obtained consecutively and reconstructed into a CT volume as the C-arm rotated 270°.

The catheter tip was visualized as a red cylinder in the 3D image on the navigation screen. With real-time tracking, the catheter was maneuvered in front of the cuff of the main stent-graft as seen in the 3D image on the navigation screen (Fig. 5A). The preshaped and relatively stiff catheters made it difficult to enter the stent-graft cuff inside the aneurysm sac. Therefore, a guidewire was blindly inserted into the stent-graft. Moving the patient under the C-arm and rotating the J-shaped tip of the guidewire freely during fluoroscopy confirmed the correct location of the guidewire within the stent-graft before the tracked catheter was pushed over the guidewire. If the guidewire was correctly located, the patient was moved back into the EM field and the catheter was pushed over the guidewire and into the stent-graft (Fig. 5B). Any guidewire that was misplaced outside the main stent-graft was retracted, and the procedure was repeated until the tracked catheter

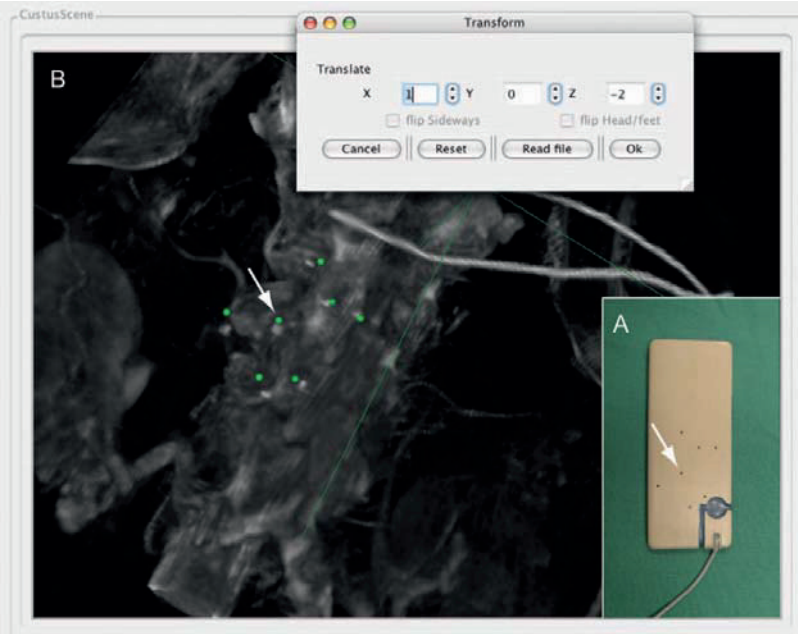

Figure 4 ◆ (**A**) The reference plate contained two 5-DOF sensors that were utilized as one 6-DOF sensor, giving both the position and orientation of the reference plate in the EM field. In addition, 7 metal spheres (arrow) were embedded in a known configuration, making it possible to visualize the 7 spheres (instead of the sensors) as green dots on the navigation screen. (**B**) The reference plate was used to manually register the CT volume to the EM field. The CT volume was moved until the radiopaque spheres in the CT image covered the corresponding green dots in the EM field. In this figure, the spheres in the CT image are not perfectly aligned with the green dots to better illustrate the registration process.

was aligned in front of the cuff or until 15 minutes had elapsed. If the guidewire and catheter were not correctly placed inside the stent-graft within 15 minutes, the catheter was changed, and the second limb was placed under regular fluoroscopic guidance, i.e., in the same manner as for the control group.

Measurements and Statistical Analysis

The following procedure variables were collected for each patient in both the intervention and the control groups: total amount of contrast medium, total amount of applied radiation in μGym^2, total procedure time, and the number of catheter repositionings and guidewire insertions required to successfully cannulate the main stent-graft in the 15-minute time limit. The data are presented as the mean $\pm$ standard deviation and median. Variables were compared using the Mann-Whitney U test in SPSS software (version 18.0; IBM Corporation, Somers, NY, USA). $P<0.05$ was indicated the threshold of significance.

RESULTS

Successful placement of the catheter inside the main stent-graft within 15 minutes was achieved in 6 (86%) of 7 patients in the intervention group and in 8 of 10 patients in the control group. Among the successfully cannulated cases (Table, Fig. 6), the maximum number of attempts required to insert the guidewire correctly was 8 in the intervention group vs. 33 in the control group

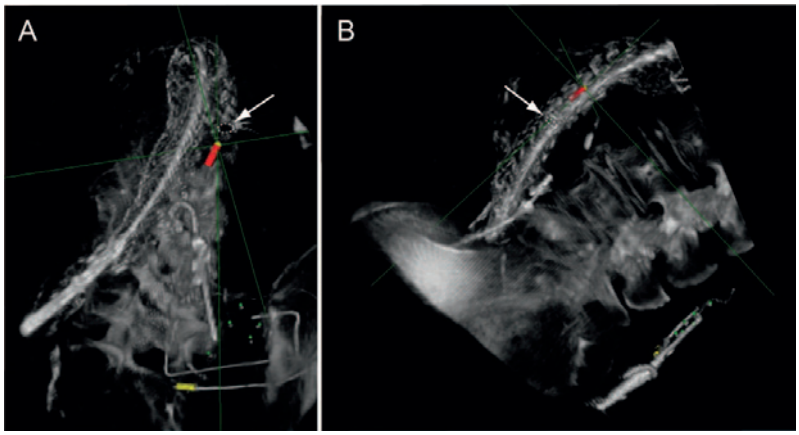

Figure 5 ◆ (**A**) The electromagnetically-tracked catheter, visualized as a red cylinder in the 3D image, was navigated in front of the contralateral cuff in the main stent-graft (arrow). When the catheter tip was in place, a guidewire was blindly inserted into the stent-graft. (**B**) After correct guidewire insertion was verified by fluoroscopy, the tracked catheter was advanced into the stent-graft over the guidewire. The correct location (arrow) inside the stent-graft is seen in the 3D image.

(p=0.059). Although the amount of contrast used (p=0.950) and total procedure time (p=0.108) were similar in the intervention and control groups, the total radiation dose (p=0.043) was higher in the intervention group. In the unsuccessful case in the intervention group, the catheter could not be placed in front of the cuff despite numerous attempts with different catheter shapes, probably due to a severely tortuous iliac artery combined with the stiffness of the catheters.

DISCUSSION

While the Aurora EM tracking system has been thoroughly assessed in regard to real-time updating, accuracy, robustness, and working volume,[9] the current feasibility study provided valuable insight into how this 3D EM navigation system behaves in vivo in the angiography suite. In the successful procedures, fewer attempts were needed to insert the guidewire and catheter correctly into the main stent-graft in the intervention group, even though the guidewire was inserted blindly. Although the contrast dosage was similar in the intervention and control groups, the total radiation dose and total procedure time were higher in the intervention group. However, these variables include the extra time spent acquiring the CT scan and testing the novel navigation technology. In the present study, the intraoperative CT

TABLE
Comparison of Parameters for Successful Procedures Within 15 Minutes

	Intervention Group (n=6)	Control Group (n=8)	p
Procedure time, min	141±24 (147)	118±24 (107)	0.108
Radiation, μGym^2	27,376±9,239 (27,100)	16,959±6,057 (17,793)	0.043
Contrast, mL	232±66 (253)	243±69 (250)	0.950
Time to insert guidewire, min	7.0±2.8 (6.0)	5.3±4.0 (3.0)	0.282
Attempts to insert guidewire	4.2±2.8 (4.5)	14.4±12.4 (8.5)	0.059

Data are presented as the means ± standard deviation (median).

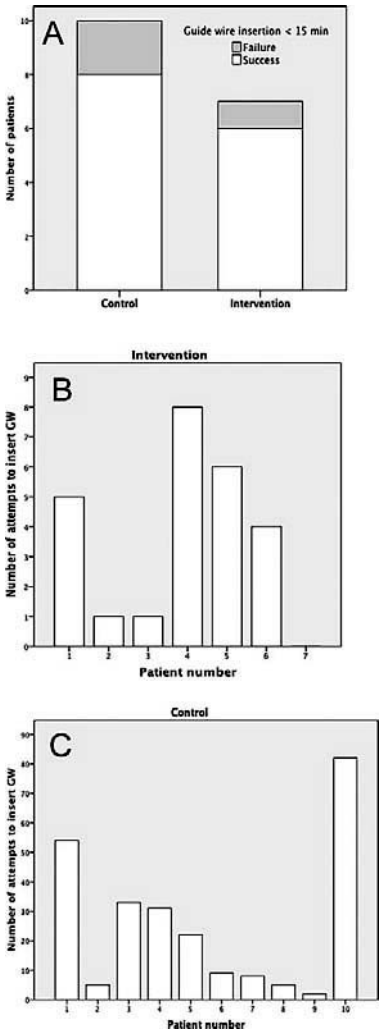

Figure 6 ◆ (**A**) The number of patients with successful insertion of a regular catheter (control group) or an electromagnetically-tracked catheter (intervention group) into the main stent-graft within 15 minutes. (**B**) When the electromagnetically-tracked catheter was placed in a satisfactory position in front of the stent-graft cuff, no more than 8 attempts were needed to insert the guidewire into the cuff, even though this was done blindly. In the seventh patient, the radiologist was not able to properly place the tracked catheter, so no guidewire was inserted within the 15-minute limit. (**C**) In general, more attempts were needed to insert the guidewire into the main stent-graft in the control group. For the first and last patients, the 15-minute time limit to insert the guidewire was exceeded. GW: guidewire.

scans were acquired without contrast, but the additional radiation from a single contrast-enhanced CT scan during an infrarenal EVAR procedure usually constitutes a modest share of the total amount of radiation applied.[10] We anticipate that the navigation system, when employed by interventional radiologists with experience in using navigation technology, will help reduce the procedure time and the demand for contrast and radiation, not only in complex procedures with prolonged operation times but also in the traditional and simpler procedures.

The tip of the custom-made, electromagnetically-tracked catheters was pre-shaped in different angles according to the vascular anatomy of the patients. However, the catheters were relatively rigid, and most patients had tortuous iliac vessels. The reduced flexibility of the catheters made it difficult to place a catheter correctly in front of the contralateral cuff in some patients. In the last patient in the intervention group, the tortuous iliac artery and the lack of catheter maneuverability prevented the radiologist from inserting the guidewire within the 15-minute limit. More flexible and steerable catheters that better cope with tortuous anatomy would clearly have simplified the navigation and improved the benefits of navigation technology in the present study.

When a catheter is placed in front of the stent-graft cuff under fluoroscopy, its location must be verified in the lateral and anterior-posterior plane at a minimum; in daily practice, this requires repeated attempts at cannulation with the C-arm in one position. This is not necessary when a 3D image is used for navigation; the spatial information is available at any time. The radiologists using the 3D EM navigation system soon became familiar with the new technology and visualization technique. When presenting a 3D image on a 2D navigation screen, it can sometimes be

difficult to comprehend the location of the tool in use. Therefore, 3 smaller images, showing the orthogonal CT slices, were presented next to the 3D navigation image on the navigation screen. The 3D navigation image could also be rotated along all 3 axes for continuous adjustment and to display the optimal view.

The 3D EM navigation system has obvious benefits and should be applicable to all types of endovascular aortic repairs, particularly procedures that are more technically challenging, such as in TAAAs and juxtarenal aneurysms. In these types of cases, the doses of contrast and radiation accumulate, as the visceral arteries have to be sufficiently displayed and often cannulated. In TAAA repair, the cannulation of branch vessels through fenestrations and directional cuffs with normal catheters can be cumbersome. The presence of tortuous arteries, thrombi, and vessel calcifications further complicate the cannulation of visceral branches, which might be simplified by the use of steerable and electromagnetically-tracked catheters. Riga et al.[11,12] investigated whether robotic endovascular catheters (REC) under fluoroscopic guidance enhanced visceral vessel cannulation in phantom models. They reported that RECs were best suited for challenging anatomical configurations, providing reduced operation time and fewer catheter movements. In their first attempt using RECs in EVAR, Riga and colleagues[13] were successful in navigating a 14-F remotely steerable robotic catheter through the aneurysm sac, cannulating the contralateral cuff of a bifurcated stent-graft under fluoroscopic guidance, and placing stiff guidewires using fine and controlled movements.

An electromagnetically-tracked guidewire might be better suited to cannulate a stent-graft than an electromagnetically-tracked catheter when a 3D EM navigation system is used. However, when the present study was performed, the available prototype sensors were too fragile to ensure proper functioning during guidewire manipulation, which is why tracked guidewires were not used in our study. However, a sensor integrated into the tip of a catheter is relatively simple to produce, so company-manufactured guidewires and catheters with integrated sensors will significantly reduce sensor fragility and will be even more practical and user-friendly for guidance of EVAR. A 3D EM navigation system integrated in the angiography suite and used in combination with industry-manufactured devices might improve existing routine procedures as well as work flow in the angiography suite. We are now working on the next rational step: testing the 3D EM navigation system for guidance of endovascular procedures in combination with electromagnetically-tracked guidewires and steerable catheters.

Conclusion

This study has shown that 3D EM navigation is a feasible technology for guidance during EVAR in a clinical setting. However, the navigation technology would benefit from further refinement and more flexible tools, such as electromagnetically-tracked catheters and guidewires, to cope with tortuous vessel anatomy and to improve user-friendliness in the angiography suite. The technology is promising, but larger clinical studies are required.

Acknowledgments: The authors wish to thank Asbjorn Odegard, Department of Radiology, St Olavs Hospital, Trondheim, Norway, for his valuable and insightful opinions, and Stein Erik Dorum, Department for Medical Technology, St Olavs Hospital, for manufacturing the electromagnetically-tracked catheters.

REFERENCES

1. Reilly LM, Chuter TA. Endovascular repair of thoracoabdominal aneurysms: design options, device construct, patient selection and complications. *J Cardiovasc Surg (Torino)*. 2009; 50:447–460.
2. Greenberg RK, Lytle B. Endovascular repair of thoracoabdominal aneurysms. *Circulation*. 2008; 117:2288–2296.
3. Geijer H, Larzon T, Popek R, et al. Radiation exposure in stent-grafting of abdominal aortic aneurysms. *Br J Radiol*. 2005;78:906–912.
4. Jones C, Badger SA, Boyd CS, et al. The impact of radiation dose exposure during endovascular aneurysm repair on patient safety. *J Vasc Surg*. 2010;52:298–302.
5. McCullough PA, Adam A, Becker CR, et al. Risk prediction of contrast-induced nephropathy. *Am J Cardiol*. 2006;98:27K–36K.

6. Manstad-Hulaas F, Ommedal S, Tangen GA, et al. Side-branched AAA stent-graft insertion using navigation technology: a phantom study. *Eur Surg Res*. 2007;39:364–371.
7. Manstad-Hulaas F, Tangen GA, Gruionu LG, et al. Three-dimensional endovascular navigation with electromagnetic tracking: ex vivo and in vivo accuracy. *J Endovasc Ther*. 2011;18:230–240.
8. Abi-Jaoudeh N, Glossop N, Dake M, et al. Electromagnetic navigation for thoracic aortic stent-graft deployment: a pilot study in swine. *J Vasc Interv Radiol*. 2010;21:888–895.
9. Yaniv Z, Wilson E, Lindisch D, et al. Electromagnetic tracking in the clinical environment. *Med Phys*. 2009;36:876–892.
10. Eide KR, Ødegård A, Myhre HO, et al. DynaCT during EVAR – a comparison with multidetector CT. *Eur J Vasc Endovasc Surg*. 2008;37:23–30.
11. Riga CV, Cheshire NJ, Hamady M, et al. Robotic endovascular catheters (REC) improve accuracy, reduce time and minimise radiation exposure in complex vascular procedures. *Br J Surg*. 2009;96:7.
12. Riga CV, Cheshire NJ, Hamady MS, et al. The role of robotic endovascular catheters in fenestrated stent-grafting. *J Vasc Surg*. 2010;51:810–820.
13. Riga C, Bicknell C, Cheshire N, et al. Initial clinical application of a robotically steerable catheter system in endovascular aneurysm repair. *J Endovasc Ther*. 2009;16:149–153.